C.P. No. 349
(18,211)
A R.C. Technical Report

C.P. No. 349
(18,211)
A.R.C. Technical Report

MINISTRY OF SUPPLY

AERONAUTICAL RESEARCH COUNCIL

CURRENT PAPERS

Investigation of High Length/Beam Ratio Seaplane Hulls with High Beam Loadings

Hydrodynamic Stability Part 20

The Effect of Slipstream on Stability and Spray Characteristics

By

D. M. Ridland, A.F.R.Ae.S., G.I.Mech.E.

LONDON HER MAJESTY'S STATIONERY OFFICE

1957

PRICE 7s 6d NET

Current Paper No. 349
Report No. F/Res/256
September, 1955

MARINE AIRCRAFT EXPERIMENTAL ESTABLISHMENT, FELIXSTOWE, SUFFOLK

INVESTIGATION OF HIGH LENGTH/BEAM RATIO SEAPLANE HULLS WITH HIGH BEAM LOADINGS

HYDRODYNAMIC STABILITY PART 20

THE EFFECT OF SLIPSTREAM ON STABILITY AND SPRAY CHARACTERISTICS

by

D. M. Ridland, A.F.R.Ae.S., G.I. Mech. E.

SUMMARY

The effects of slipstream on longitudinal stability, spray and elevator effectiveness are deduced from tests on four configurations of the basic model of the series which differed only in aerodynamic details.

It was found that in general increases in thrust coefficient improved longitudinal stability, spray characteristics and elevator effectiveness. A method of applying the detailed results to the stability limits of other models of the series is outlined.

/ LIST OF CONTENTS

LIST OF CONTENTS

LIST OF TABLES

/ LIST OF FIGURES

LIST OF FIGURES

/ 1. INTRODUCTION

1. INTRODUCTION

In this report results are given of tests made to determine the effects of slipstream on the hydrodynamic longitudinal stability and spray characteristics of Model A, the basic model of the series detailed in Reference 1, a list of which is reproduced in Table I. Full details are given in this reference of the considerations affecting the design of the models, but it may be mentioned here that Model A has a length/beam ratio of 11 (the forebody being 6 beams in length and the afterbody 5 beams), an afterbody to forebody keel angle of 6° and a straight transverse step with a step depth of 0.15 beams; it has no forebody warp, no effective afterbody warp and no step fairing. The differences between the configurations used in the present tests are purely aerodynamic, the hull, tail unit and basic mainplane being identical in each case. The hull lines of the model are given in Figure 1 and photographs of the four test configurations (which are described below) are given in Figure 2; relevant hydrodynamic and aerodynamic data are given in Tables I and II respectively. The techniques used in the tests and the presentation of results, together with the reasons for using them, are considered in References 1 and 2, though a brief summary is given below.

The configurations tested may be described briefly as being

(i) with take-off power,
(ii) with fairings replacing propellers,
(iii) with propellers windmilling, and
(iv) with full span leading edge slats (and no propellers, fairings or nacelles).

Results of tests on the first three of these configurations, all fitted with nacelles, show the general effects of slipstream on the stability and spray characteristics of a high length/beam ratio hull, while comparison of these results with those of the last configuration[3] (the standard test configuration) enable the slipstream characteristics to be related to the models of the main series. Tests with slipstream were not made on each model, in order to save testing time.

2. DETAILS OF TEST CONFIGURATIONS

The following details of the test configurations are given both for convenience and to amplify the information in Reference 1, and a general view of each configuration is given in Figure 2.

(i) With take-off power

The 1/15 scale Sunderland mainplane, common to each model of the series, was fitted with four turbine-propeller units; the turbines were Mk.IIb compressed air turbines (Reference 20) and the propellers were 0.795 ft. in diameter. Leading edge slats were fitted outboard of the outer nacelles, the arrangement being shown in some detail in Figure 1 of Reference 1. The units were supplied with compressed air at constant pressure to give take-off thrusts of the right order for this type of hull. The resulting variation of thrust with speed is shown in Figure 11 of Reference 1 and the thrust coefficient (T_c) - speed relationship is given in Figure 3 of the present report. The mean thrust line was inclined upwards at 3° 9' to the hull datum (tangent to forebody keel at step) and its distance from the C.G. measured normal to the thrust line was 0.28 ft. The pitching moment of inertia of the model in this configuration was 23.25 lb. ft.^{2}.

(ii) With propellers windmilling

This configuration was exactly the same as (i), except that no air pressure was supplied to the turbines.

/ (iii)

(iii) With fairings

In this configuration the propellers and turbines of (i) were removed; dummy engines (weights) were placed inside the nacelles to maintain the pitching moment of inertia at 23.25 lb. ft.^{2} and fairings were fitted in place of the propellers.

(iv) With full span slats

In this case the turbines, propellers and nacelles of (i) were removed, the compressed air outlets to the turbines were plugged and pared down to leave a smooth wing leading edge and full span leading edge slats were fitted; a good view of the wing in this state is given in Figure 2 of Reference 1. This wing configuration is the standard one and was used throughout the main investigation for the routine tests on each model; the results of such tests on Model A are reported in Reference 3. The reduced pitching moment of inertia of Model A with full span slats was 20.90 lb. ft.^{2}.

3. DESCRIPTION OF TESTS

3.1. General

All tests were made with a load coefficient of 2.7, one C.G. position, zero flap and at steady speeds only.

3.2. Lift

Lift runs were in general made at constant fixed speed with the model clear of the water, over a range of attitudes with $\eta = 0^\circ$. A limited number of runs was made at different speeds to check Reynolds Number effects, and the effect of elevator was determined at four attitudes. In the case with take-off power the whole procedure was repeated at three additional speeds to determine the effect on lift of changes in thrust coefficient. The resulting curves for each configuration are given in Figures 4a to 4d.

3.3. Longitudinal Stability

Longitudinal stability tests were made by towing the model from the wing tips on the lateral axis through the centre of gravity, the model being free in pitch and heave. The value of the elevator setting was selected before each run, and the model towed at constant speed. The angle of trim was noted in the steady condition, and if the model proved stable at the speed selected it was given nose-down disturbances to determine whether instability could be induced, the amount of disturbance given to cause instability being in the range of 0 - 10° except in the case of tests with fairings when the maximum disturbances were limited to 5°. (The tests on Model A with fairings were made before the maximum disturbance technique was decided on and it was not practical to repeat them.) The motion was classed as unstable whenever the double amplitude of porpoising was greater than 2°. The stability limits built up by these methods together with the corresponding trim curves are given for each configuration in Figures5a to 6d. The limits are compared on a C_V base in Figure 7, on a $\sqrt{C_\Delta}/C_V$ base in Figure 8 and they are plotted with elevator angles as ordinates in place of keel attitudes in Figure 9. The load coefficient curves, which are necessary for the transposition to a $\sqrt{C_\Delta}/C_V$ base, are given in Figures 10a to 10d and trim curves for $\eta = 0^\circ$ are compared in Figure 16.

3.4. Spray and Wake Formation

Photographs were taken of the spray, from three different positions, over a range of speeds and with elevators set at -8°. A number of these photographs are reproduced in Figures 12a to 12c for the configurations with take-off power, with propellers windmilling and with fairings; similar photographs for the configuration with full span slats are given in Reference 3. They have been used to determine the projections of the spray envelopes on the plane of

/ symmetry

symmetry of the model for the different configurations, and these projections are plotted in Figure 13. This method of plotting differs from that originally proposed (Reference 1) but it is felt to be more realistic. The absence of projections orthogonal to these, which cannot be obtained from the photographs, is not serious since the photographs enable the positions of the spray blisters to be judged qualitatively, and in any case the curves are intended for comparison purposes rather than for absolute measurements. It should be noted that in plotting the projections velocity spray has in general been ignored.

In addition to the spray photographs, photographs of the wake region for all configurations except that with fairings, were taken from two different positions and are reproduced in Figures 11a and 11b for the take-off power and propellers windmilling cases respectively; those for the case with full span slats are given in Reference 3. These photographs covered a range of speeds and elevator settings, the combinations being selected to give the maximum possible variation of wake formation and position relative to the afterbody in the stable planing region.

3.5. Elevator Effectiveness

Curves of elevator effectiveness calculated from the longitudinal stability diagrams are given in Figures 14a to 14d and compared in Figure 15.

4. DISCUSSION

4.1. Lift

As differences between the configurations are such as to affect primarily the aerodynamics of the model, the lift characteristics and the state of flow over the wing are briefly considered below. It may be remembered that the lift curves were used in the calculation of load coefficients, which in turn were used in the transposition of the stability limits to a $\sqrt{C_L}/C_V$ base, so any peculiarity in the lift characteristics will be reflected throughout the sequence. It should also be noted that the curves have been plotted on a keel attitude base so as to be directly applicable to the stability diagrams; wing incidence is 6° 9' greater than keel attitude.

The lift curves with take-off power (Figure 4a) show an increasing tendency to regularity as the thrust coefficient is decreased; at $T_C = 9.4$ the points are disorderly and only the curve for $\eta = 0°$ has been drawn, while at $T_C = 0.4$ a clear indication of the effect of elevator is given. As planing is not established until about $C_V = 4.5$, however, only the curves for $T_C < 2.0$ are significant in the present context and the transposed stability limits should be fairly accurate. The airflow past the wing will probably be mixed; at the tips it should be laminar over much of the chord, the slats preventing breakaway and delaying transition, while behind the propeller discs normal slipstream conditions will exist.

The lift curves with propellers windmilling (Figure 4b) are peculiar in that the curve for $\eta = 0°$ is of greater slope and reaches higher lift coefficients than do the curves for the other elevator settings. The loss of lift with elevator may be due to inefficiency of the tailplane at other than the zero elevator setting, as a result of the retarded flow through the propellers, or to elevator changes affecting the flow over the mainplane. (Subtraction of tailplane lift (as measured with no slipstream, Reference 1) for $\eta = 0°$ at $\alpha_K = 8°$ and 10° would give lift coefficients of 0.97 and 1.00 respectively, thereby putting the curve in place within the set. The tailplane lift curve is given in Figure 12 of Reference 1). It should be noted that this configuration may be considered as one with negative thrust and there may therefore be a variation of the lift characteristics with thrust coefficient for $T_C < 0$. This should be small, however, and the transposed stability limits should be reasonably correct.

/ The

The lift curves with fairings (Figure 4c) clearly indicate transition and associated breakaway 21, 22. The flow over the wing is thus in a critical state and likely to be affected by small changes in Reynolds Number. The associated load coefficients can therefore only be of the right order and the accuracy of the transposed stability limits will suffer accordingly.

The lift curves with full span slats (Figure 4d) are regular and accurate; this is the result of laminar flow being maintained with little breakaway over the whole wing span by means of the leading edge slats and there should be little error in the corresponding transposition.

4.2. Longitudinal Stability

The effects of slipstream on the longitudinal stability characteristics of Model A may be determined from a detailed study of the individual stability diagrams, but it is more convenient to make separate comparisons of the limits and the trim curves.

Both undisturbed and disturbed stability limits are compared on a C_V base in Figure 7. If the curves for the case with full span slats be neglected initially, the other three cases - take-off power, fairings and propellers windmilling, taken in that order - constitute a set, viz: positive, zero and negative thrust cases respectively and illustrate, as well as the general effects of slipstream, the effects on the limits of a progressive reduction in thrust coefficient. In the undisturbed case these are to increase both the speeds and attitudes at which the limits are encountered. At low attitudes the lower limits converge and at high attitudes there is a minor exception to the foregoing rule in the case with propellers windmilling, but this is not significant. In the disturbed case the same type of pattern can be seen, although it is modified slightly because of the different limits involved. (It may be remembered that the disturbed limit for the case with fairings was obtained with only 5° disturbance. The part of the limit drawn should only be altered slightly by the application of the maximum disturbance technique[23] however, and may thus be usefully included in this comparison). The progressive movement of the limits up the speed scale with decrease of T_c is much greater than in the undisturbed case, while the attitude changes are about the same.

By comparing individually the undisturbed and disturbed limits for each thrust case, the changes in disturbance effects following general variations in thrust coefficient can be ascertained. With positive thrust or take-off power the effects of disturbance are to double the vertical band of instability found across the take-off path without disturbance and to raise the high speed part of the lower limit, with zero thrust or fairings the disturbance effects are greater the vertical band being more than doubled, while in the negative thrust case disturbance causes the onset of instability over almost the whole of the planing speed range; there is thus a rapid worsening of disturbance effects with decrease in thrust coefficient. This means that during landing an aircraft is far more susceptible to disturbance than during take-off. (It is felt that this conclusion is a general one and is not peculiar to this hull form.)

The limits obtained with full span slats lie in general with the limits for the cases with propellers windmilling and fairings, away from those obtained with take-off power. They are better discussed however, in relation to the other limits, when plotted on a $\sqrt{C_\Delta}/C_V$ base (Figure 8) which relates waterborne load to speed [24], i.e. which accounts directly for changes in lift and indirectly for changes in pitching moment when these may be likened, as in the present case, to a change in elevator setting. The object of these tests with respect to the full span slat configuration is to assess the magnitude and character of the changes effected by take-off power and windmilling propellers in the case of models of this series. The effects in the case of Model A are readily observed from Figures 7 and 8; their application to the other models is considered below.

/ The

The hulls concerned are of the same family, differing only in the hull parameter under investigation, and differences in loading and trim are taken account of by the method of plotting. It follows that any difference between the magnitude of the slipstream effects for Model A (Figure 8) and those for any other model of the series will be due entirely to the effect of the hull parameter which has been varied in going from one model to the other; in other words to some ancillary effect. The magnitude of this effect may of course be affected by the specific values of the hull parameters which are the same for the two models. Where such ancillary effects are small therefore the effects of slipstream and windmilling propellers may be taken to be the same as in the case of Model A. For instance, the lower undisturbed stability limits for most of the models with unwarped forebodies collapse on that for Model A when plotted on a $\sqrt{C_\Delta}/C_V$ base [19]; the secondary effects are therefore small and slipstream effects will be sensibly the same in each case. Upper limit changes will have to be applied with discretion and only the general nature of the effects can be considered in the disturbed case. It is felt that with a suitable redefinition of hull attitude the foregoing will also apply with small error to the warped forebody cases.

It is interesting to note that in Figure 8 the limits for the cases with full span slats and propellers windmilling form a set which is separated from the remainder, which form another set, and that the general pattern of the undisturbed limits is reflected in some detail in the arrangement of disturbed limits.

The plots of stability limits with elevator angles replacing keel attitudes as ordinates in Figure 9 are given mainly for information. It may be noted however, that in the undisturbed case the lower limits obtained with take-off power and windmilling propellers are separated from those for the full span slat case by negative and positive amounts of elevator respectively. This is consistent with the representation of the additional thrust moments by a change in elevator setting, but the idea cannot be taken far, without consideration of differences in elevator efficiency and in the actual stability limits.

The effects of slipsteam on trim are shown in Figure 16, where the curves for $\eta = 0^0$, which have been taken as typical, are compared. As would be expected they lie in order, the highest attitudes being reached on the trim curves with the lowest forward thrust, and this inverse relationship is preserved throughout the take-off speed range. The spacing of the curves is almost constant over the planing speed range, but it should be noted that while the increase in attitude with decrease in thrust is progressive, it varies with speed and is non-linear. Comparison of other trim curves shows that the inverse variation of trim with thrust coefficient is found at all elevator settings, but the spacing of the curves varies, the distribution being more even at high values of elevator angle and less so at low values.

The trim curves for the cases with fairings and full span slats in Figure 16 lie together, indicating that only a small amount of drag is obtained from the faired nacelles.

4.3. Wake Formation

As the photographs of the wake regions are of representative rather than specific cases they can only be compared individually in isolated instances, that is when speeds and attitudes are approximately equal. Where this can be done, which is in the full span slat and windmilling propellers cases only, there are no noticeable differences in wake characteristics.

Taken as groups, the photographs give the same general impression in each case, there being no major differences between the configurations. With take-off power, however, the flow at the lower speeds does appear to be more broken than in the other cases, but this effect is not well defined.

/ Although

Although no photographs were taken of flow in the wake region in the case with fairings, it is felt that such photographs would not differ appreciably from those for the full span slat configuration.

4.4. Spray.

The effects of slipstream on spray are best considered by adopting the method used in the comparison of longitudinal stability limits. Neglecting initially therefore the full span slat case and considering the spray photographs for the configurations with take-off power, fairings and windmilling propellers respectively the effects on spray of a progressive reduction in thrust coefficient can be seen at each speed.

In general, with reduction of thrust coefficient there is an increase in the height of the spray blister and, while with zero thrust there is an unbroken and apparently undisturbed blister, in the cases with positive and negative thrust the spray is, or tends to be, sucked into the propellers and broken up. These points are illustrated in the photographs for individual speeds. Those for $C_v = 1$ are of little consequence as in the negative thrust configuration at this speed friction in the system is preventing the propellers from turning. At $C_v = 2$ the relative heights of the spray profiles can be clearly seen together with the raising and breaking of the blister in the positive thrust case. At $C_v = 3$ in the case with negative thrust there appears to be a suction at some distance behind the propeller plane, which distorts and raises the blister, while with positive thrust the suction occurs either in the propeller plane or just in front of it. Photographs for the higher speeds are not quite so instructive, except perhaps for the rear views at $C_v = 4$. The relative positions of the spray profiles are clearly shown here, but that for the positive thrust case is disturbed just below the wing trailing edge and indicates depression by the slipstream.

It should be noted that as in the negative thrust case the propeller drag is a function of the forward speed and the thrust coefficient will probably vary only a small amount, and as in the positive thrust case the thrust coefficient varies greatly at low speeds, the separation of the three sets of photographs in terms of thrust coefficient will vary with speed, being most uneven at the lowest speed, and this should be borne in mind when examiningthe photographs.

The projections of the envelopes of the spray profiles in Figure 13 show the decrease in spray height with increase of thrust coefficient, except at high values of C_x where the positive thrust curve rises across the others. This is undoubtedly due to the reduction in attitude and consequent movement forward of the spray origin which occurs at low speeds with positive thrust.

4.5. Elevator Effectiveness

The comparison of curves of mean elevator effectivenss (Figure 15) shows that with a progressive general increase in thrust coefficient there is an increase in mean elevator effectiveness and, except in the case with positive thrust, the effect is sensibly constant over the planing range of speeds; with positive thrust the increase in effectiveness with speed is reduced at the higher speeds. The curve for the full span slat configuration lies a little above that for the case with fairings.

In considering these curves it should be noted that, at a given speed, an increase in thrust coefficient will have two main effects viz: the load on water will be reduced, which effect by itself will produce an increase in elevator effectiveness[4], and the efficiency of the elevators and tailplane will be improved when they are in the accelerated flow of the slipstream. It would appear however, from the nature of the change, that neither of these effects is the cause of the rather sudden decrease in slope of the positive thrust curve at $C_v = 7$.

/ It

It is probable that the large nose down moment obtained with positive thrust has caused such a general reduction in trim that an effective lower limit, in the form of high opposing hydrodynamic moments, has been reached and this limit has caused a flat ending of the lower trim curves with a consequent reduction in trim range for a given speed i.e. a reduction in mean elevator effectiveness. The effect can be seen in Figure 5a, where the lower trim curves show a decrease in slope at speed coefficients greater than 7.

A comparison of the relevant load coefficients, on a basis of either constant elevator angle ($\eta = -8^{\circ}$) or attitude ($\alpha_k = 8^{\circ}$), shows that at the higher speeds the loads on water obtained with positive thrust are about half those obtained with negative thrust, and while as would be expected, the case with slats lies in between these two, that with fairings gives the greatest loads at all planing speeds. These high water loads with fairings are a direct result of the loss of lift with transition and associated breakaway and, as they constitute the major difference between this and the full span slat configuration (both are zero thrust cases) elevator effectiveness should be slightly greater at all speeds with slats than with fairings, which in fact it is. The low values of elevator effectiveness obtained with negative thrust are lower than the corresponding decrease in load would indicate; it is suggested that the further loss of effectiveness is due to the inefficiency of the elevators and tailplane mentioned in Section 4.1.

5. CONCLUSIONS

The tests made show that the application of take-off power results in a general improvement in both the stability and spray characteristics of a high length/beam ratio hull. The detailed effects of a progressive and general increase in thrust coefficient are

(i) to reduce both the speeds and attitudes at which stability limits without disturbance are met,

(ii) to reduce both the speeds and attitudes at which stability limits with disturbance are met, the decrease in speed being much greater than in (i),

(iii) to increase resistance to disturbance,

(iv) to reduce trim throughout the take-off range of speeds, the reduction being much greater in the planing than in the displacement range of speeds,

(v) to lower the spray blister generally, which results in a lower spray envelope except at very low speeds and

(a) with increase in T_c from zero, to raise the blister locally near the propeller plane with the spray sheet ultimately being broken and sucked into the propellers and,

(b) with increase in T_c to zero, to reduce the local distortion of the spray sheet behind the propeller plane until at $T_c = 0$ the undisturbed blister is obtained,

(vi) to increase elevator effectiveness and

(vii) to reduce the elevator setting at which lower limit, undisturbed instability is encountered.

/ The

The above conclusions can be applied to obtain a fair idea of the effects of slipstream on the stability and spray characteristics of any model of the present series. A better estimate can be made however, in the case of stability limits only, by plotting the limits on a $\sqrt{C_A}/C_m$ base together with those for model A in the corresponding configuration; where a collapse is obtained the results for model A can be applied directly. This will occur mainly in the case of the lower limit without disturbance, leaving the upper limit without disturbance and the disturbed limit cases to be interpreted in the light of the general conclusions.

*Action copy.

/ LIST OF SYMBOLS

LIST OF SYMBOLS

b	beam of model
C_L	lift coefficient = $L/\frac{1}{2}\rho SV^2$ (L = lift, ρ = air density)
C_V	velocity coefficient = $V/\sqrt{gb}$
C_Δ	load coefficient = Δ/wb^3 (Δ = load on water and w = weight per unit volume of water)
C_{Δ_o}	load coefficient at $V = 0$
C_X	longitudinal spray coefficient = x/b
C_Y	lateral spray coefficient = y/b
C_Z	vertical spray coefficient = z/b
	(x,y,z) co-ordinates of points on spray envelope relative to axes through step point
S	gross wing area
V	velocity
α_K	keel attitude
η	elevator setting
T_c	thrust coefficient = $T/\rho V^2 d^2$ (T = thrust, d = propeller diameter).

/ LIST OF REFERENCES

LIST OF REFERENCES

No.	Author(s)	Title
1	D. M. Ridland J. K. Friswell A. G. Kurn	Investigation of High Length/Beam Ratio Seaplane Hulls with High Beam Loadings: Hydrodynamic Stability Part 1: Techniques and Presentation of Results of Model Tests. Current Paper No. 201. September 1953.
2	J. K. Friswell A. G. Kurn D. M. Ridland	Investigation of High Length/Beam Ratio Seaplane Hulls with High Beam Loadings: Hydrodynamic Stability Part 2: The Effect of Changes in the Mass, Moment of Inertia and Radius of Gyration on Longitudinal Stability Limits. Current Paper No. 202. September 1953.
3	D. M. Ridland J. K. Friswell A. G. Kurn	Investigation of High Length/Beam Ratio Seaplane Hulls with High Beam Loadings: Hydrodynamic Stability Part 3: The Stability and Spray Characteristics of Model A. M.A.E.E. Report F/Res/237. February 1954.
4	D. M. Ridland A. G. Kurn J. K. Friswell	Investigation of High Length/Beam Ratio Seaplane Hulls with High Beam Loadings: Hydrodynamic Stability Part 4: The Stability and Spray Characteristics of Model B. M.A.E.E. Report F/Res/238. March 1954.
5	J. K. Friswell D. M. Ridland A. G. Kurn	Investigation of High Length/Beam Ratio Seaplane Hulls with high Beam Loadings: Hydrodynamic Stability Part 5: The Stability and Spray Characteristics of Model C. M.A.E.E. Report F/Res/239. October 1953.
6	D. M. Ridland	Investigation of High Length/Beam Ratio Seaplane Hulls with High Beam Loadings: Hydrodynamic Stability Part 6: The Effect of Forebody Warp on Stability and Spray Characteristics. Current Paper No. 203. May 1954.
7	J. K. Friswell	Investigation of High Length/Beam Ratio Seaplane Hulls with High Beam Loadings: Hydrodynamic Stability Part 7: The Stability and Spray Characterisitcs of Model D. M.A.E.E. Report F/Res/241. November 1953.
8	D. M. Ridland	Investigation of High Length/Beam Ratio Seaplane Hulls with High Beam Loadings: Hydrodynamic Stability Part 8: The Stability and Spray Characteristics of Model E. M.A.E.E. Report F/Res/242. December 1953.

LIST OF REFERENCES (Contd.)

No.	Author(s)	Title
9	A. G. Kurn	Investigation of High Length/Beam Ratio Seaplane Hulls with High Beam Loadings: Hydrodynamic Stability Part 9: The Stability and Spray Characteristics of Model F. M.A.E.E. Report F/Res/243. February 1954.
10	D. M. Ridland	Investigation of High Length/Beam Ratio Seaplane Hulls with High Beam Loadings: Hydrodynamic Stability Part 10: The Effect of Afterbody Length on Stability and Spray Characteristics. Current Paper No. 204. August 1954.
11	D. M. Ridland A. G. Kurn J. K. Friswell	Investigation of High Length/Beam Ratio Seaplane Hulls with High Beam Loadings: Hydrodynamic Stability Part 11: The Stability and Spray Characteristics of Model G. M.A.E.E. Report F/Res/246. April 1954.
12	J. K. Friswell D. M. Ridland A. G. Kurn	Investigation of High Length/Beam Ratio Seaplane Hulls with High Beam Loadings: Hydrodynamic Stability Part 12: The Stability and Spray Characteristics of Model H. M.A.E.E. Report F/Res/247. February 1954.
13	D. M. Ridland	Investigation of High Length/Beam Ratio Seaplane Hulls with High Beam Loadings: Hydrodynamic Stability Part 13: The Effect of Afterbody Angle on Stability and Spray Characteristics. Current Paper No. 236. February 1955.
14	D. M. Ridland	Investigation of High Length/Beam Ratio Seaplane Hulls with High Beam Loadings: Hydrodynamic Stability Part 14: The Effect of a Tailored Afterbody on Stability and Spray Characteristics, with Test Data on Model J. Current Paper No. 351. October 1955.
15	J. K. Friswell A. G. Kurn D. M. Ridland	Investigation of High Length/Beam Ratio Seaplane Hulls with High Beam Loadings: Hydrodynamic Stability Part 15: The Stability and Spray Characteristics of Model K. M.A.E.E. Report F/Res/251. April 1954.
16	D. M. Ridland A. G. Kurn J. K. Friswell	Investigation of High Length/Beam Ratio Seaplane Hulls with High Beam Loadings: Hydrodynamic Stability Part 16: The Stability and Spray Characteristics of Model L. M.A.E.E. Report F/Res/252. April 1954.
17	J. K. Friswell D. M. Ridland A. G. Kurn	Investigation of High Length/Beam Ratio Seaplane Hulls with High Beam Loadings: Hydrodynamic Stability Part 17: The Stability and Spray Characteristics of Model M. M.A.E.E. Report F/Res/253. April 1955.

LIST OF REFERENCES (Contd.)

No.	Author(s)	Title
18	D. M. Ridland J. K. Friswell A. G. Kurn	Investigation of High Length/Beam Ratio Seaplane Hulls with High Beam Loadings: Hydrodynamic Stability Part 18: The Stability and Spray Characteristics of Model N. M.A.E.E. Report F/Res/234. April 1955.
19	J. K. Friswell	Investigation of High Length/Beam Ratio Seaplane Hulls with High Beam Loadings: Hydrodynamic Stability Part 19: The Interaction of the Effects of Forebody Warp, Afterbody Length and Afterbody Angle on Longitudinal Stability Characteristics. Current Paper No. 352. September 1955.
20	D. T. Llewelyn-Davies W. D. Tye D. C. MacPhail	The Design and Installation of Small Compressed Air Turbines for Testing Powered Dynamic Models in the Royal Aircraft Establishment Seaplane Tank. R. & M. 2620. April 1947.
21	F. W. Schmitz (Translated by M. Flint)	Aerodynamik des Flugmodells p.p. 1-63. Publishers: G. J. E. Volckmann and E. Wette, Berlin - Charlottenburg 2. (Germany). Ministry of Aircraft Production R.T.P. Translation No. 2460.
22	F. W. Schmitz (Translated by M. Flint)	Aerodynamik des Flugmodells. p.p. 63-71 and 142-159. Publishers: G. J. E. Volckmann and E. Wette, Berlin - Charlottenburg 2. (Germany). Ministry of Aircraft Production R.T.P. Translation No. 2204.
23	D. M. Ridland	Investigation of High Length/Beam Ratio Seaplane Hulls with High Beam Loadings: Hydrodynamic Stability Part 21: Some Notes on the Effects of Waves on Longitudinal Stability Characteristics. Current Paper No. 237. August 1955.
24	K. S. M. Davidson F. W. S. Locke	Some Analyses of Systematic Experiments on the Resistance and Porpoising Characteristics of Flying-boat Hulls. N.A.C.A. A.R.R. 3106. September 1943.

/ TABLE I

TABLE I

Models for hydrodynamic stability tests

Model	Forebody warp	Afterbody length	Afterbody-forebody keel angle	Step form	To determine effect of
	degrees per beam	beams	degrees		
A	0	5	6	Unfaired transverse. Step depth 0.15 beam.	Forebody warp
B	4	5	6		
C	8	5	6		
D	0	4	6		Afterbody length
A	0	5	6		
E	0	7	6		
F	0	9	6		
G	0	5	4		Afterbody angle
A	0	5	6		
H	0	5	8		
A	0	5	6		Tailored afterbody
J	0	5	6		
A	0	5	6		Interaction of parameters
D	4	5	6		
E	0	7	6		
H	0	5	8		
K	4	5	8		
L	4	7	6		
M	0	7	8		
N	4	7	8		

/TABLE II

TABLE II

Model Hydrodynamic Data

Beam at step (b)	0.475'
Length of forebody (6b)	2.850'
Length of afterbody (5b)	2.375'
Angle between forebody and afterbody keels	6°
Forebody deadrise at step	25°
Forebody warp (per beam)	0°
Afterbody deadrise	30° (decreasing to 26° at main step over forward 40% of afterbody length).
Pitching moment of inertia	
with take-off power	23.25 lb. ft.^{2}
with propellers windmilling	23.25 lb. ft.^{2}
with fairings	23.25 lb. ft.^{2}
with full span slats	22.90 lb. ft.^{2}

/TABLE III

TABLE III

Model Aerodynamic data

Mainplane	
Section	Gottingen 436 (mod.)
Gross area	6.85 sq. ft.
Span	6.27 ft.
S.M.C.	1.09 ft.
Aspect ratio	5.75
Dihedral } on 30% spar axis	3° 0'
Sweepback } on 30% spar axis	4° 0'
Wing Setting (root chord to hull datum)	6° 9'
Tailplane	
Section	R.A.F. 30 (mod.)
Gross area	1.33 sq. ft.
Span	2.16 ft.
Total elevator area	0.72 sq. ft.
Tailplane setting (root chord to hull datum)	2° 0'
Fin	
Section	R.A.F. 30
Gross area	0.80 sq. ft.
Height	1.14 ft.
General	
* C.G. position	
distance forward of step point	0.237 ft.
distance above step point	0.731 ft.
* $\frac{1}{4}$ chord point S.M.C.	
distance forward of step point	0.277 ft.
distance above step point	1.015 ft.
* Tail arm 1 (C.G. to hinge axis)	3.1 ft.
* Height of tailplane root chord L.E. above hull crown	0.72 ft.
Thrust line	
inclination upwards from hull datum	3° 9'
distance from C.G. normal to thrust line	0.28 ft.
Propeller diameter	0.795 ft.

* These distances are measured either parallel to or normal to the hull datum.

FIG. 1.

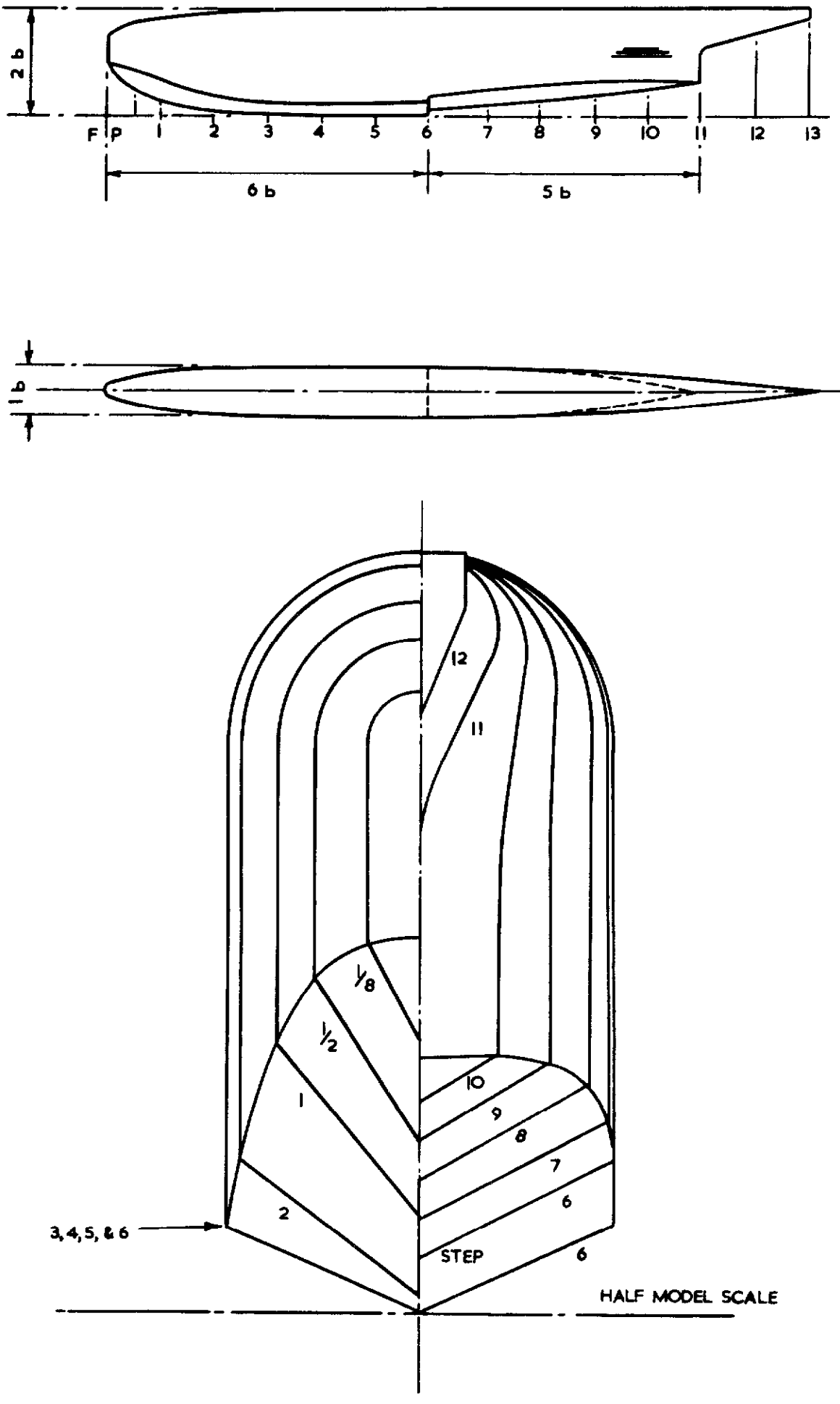

MODEL A
HULL LINES

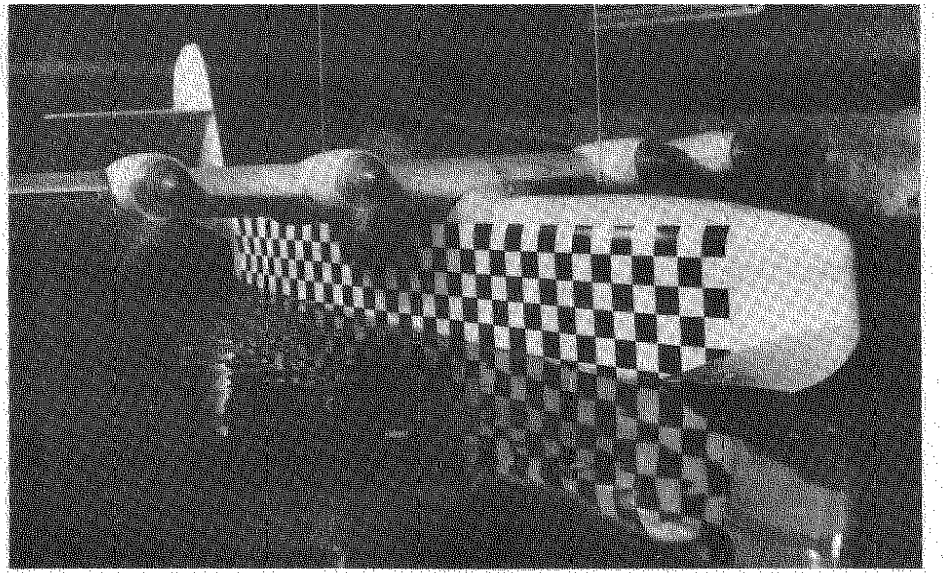

WITH TAKE - OFF POWER

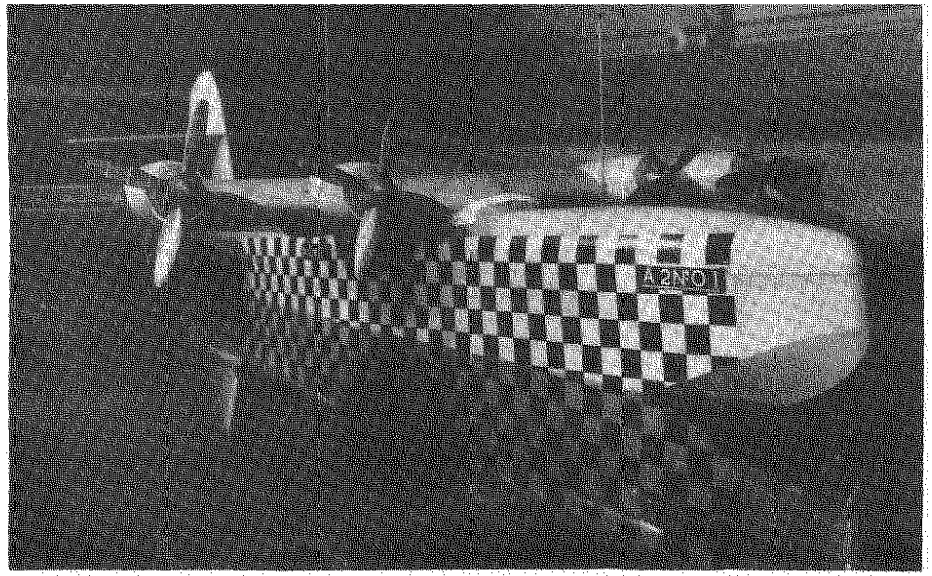

WITH PROPELLERS WINDMILLING

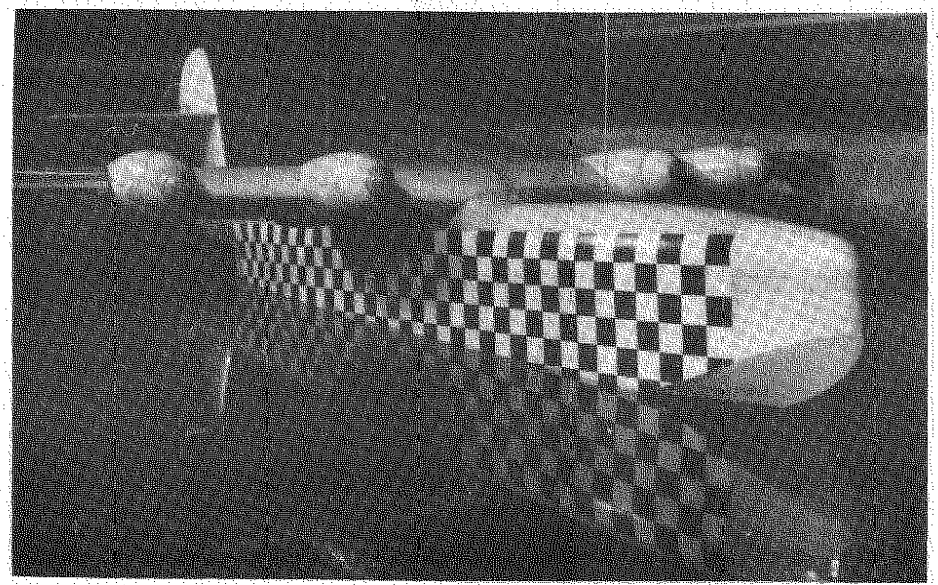

WITH FAIRINGS

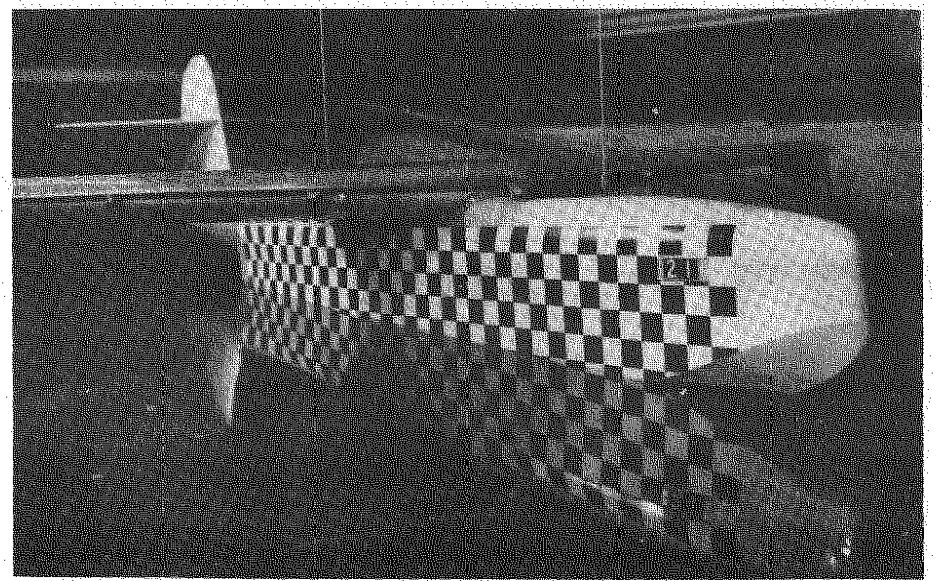

WITH FULL SPAN SLATS

PHOTOGRAPHS OF MODEL A

FIG. 2

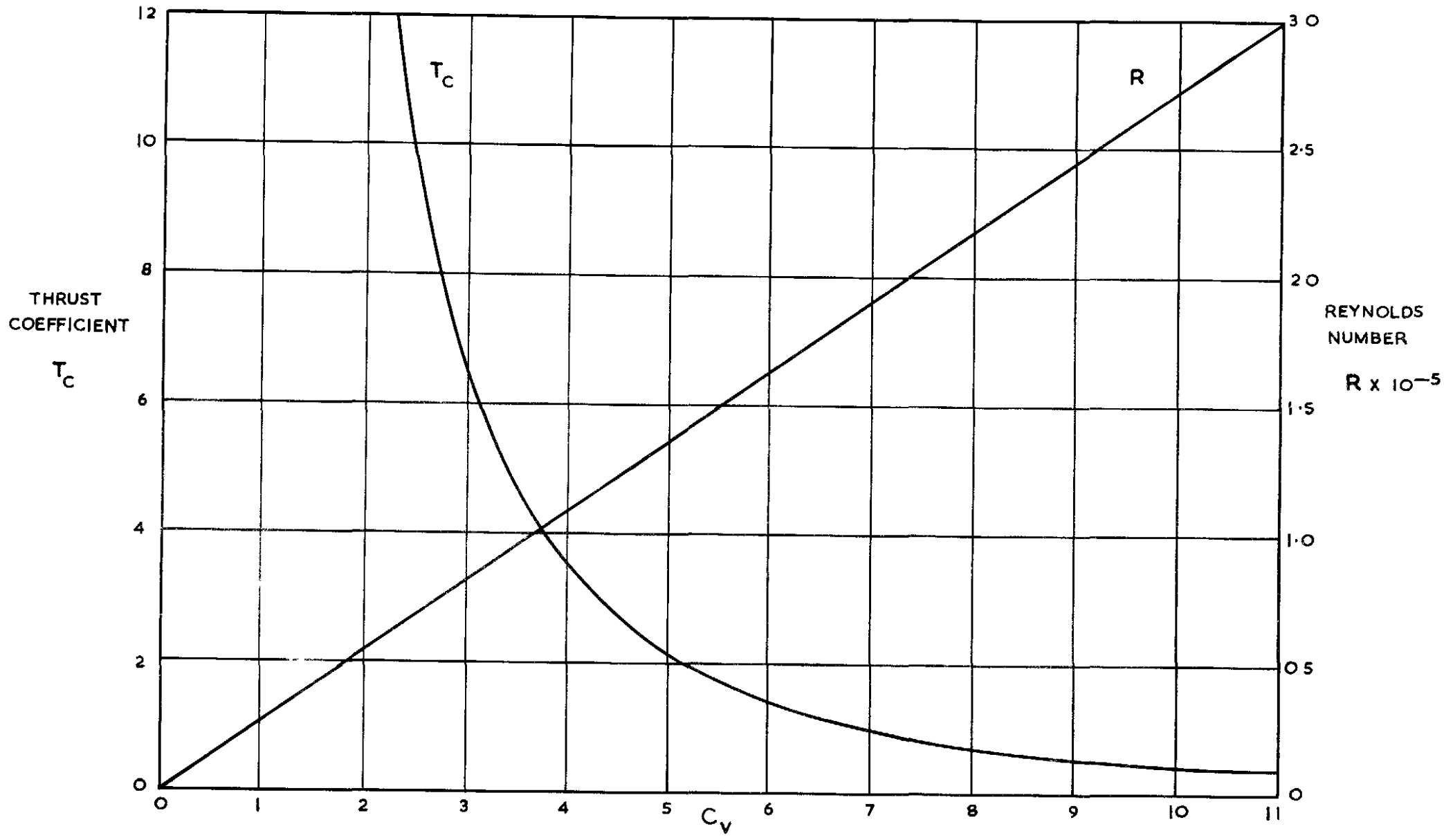

THRUST COEFFICIENT AND REYNOLDS NUMBER V VELOCITY COEFFICIENT

FIG. 3.

FIG. 4a.(1)

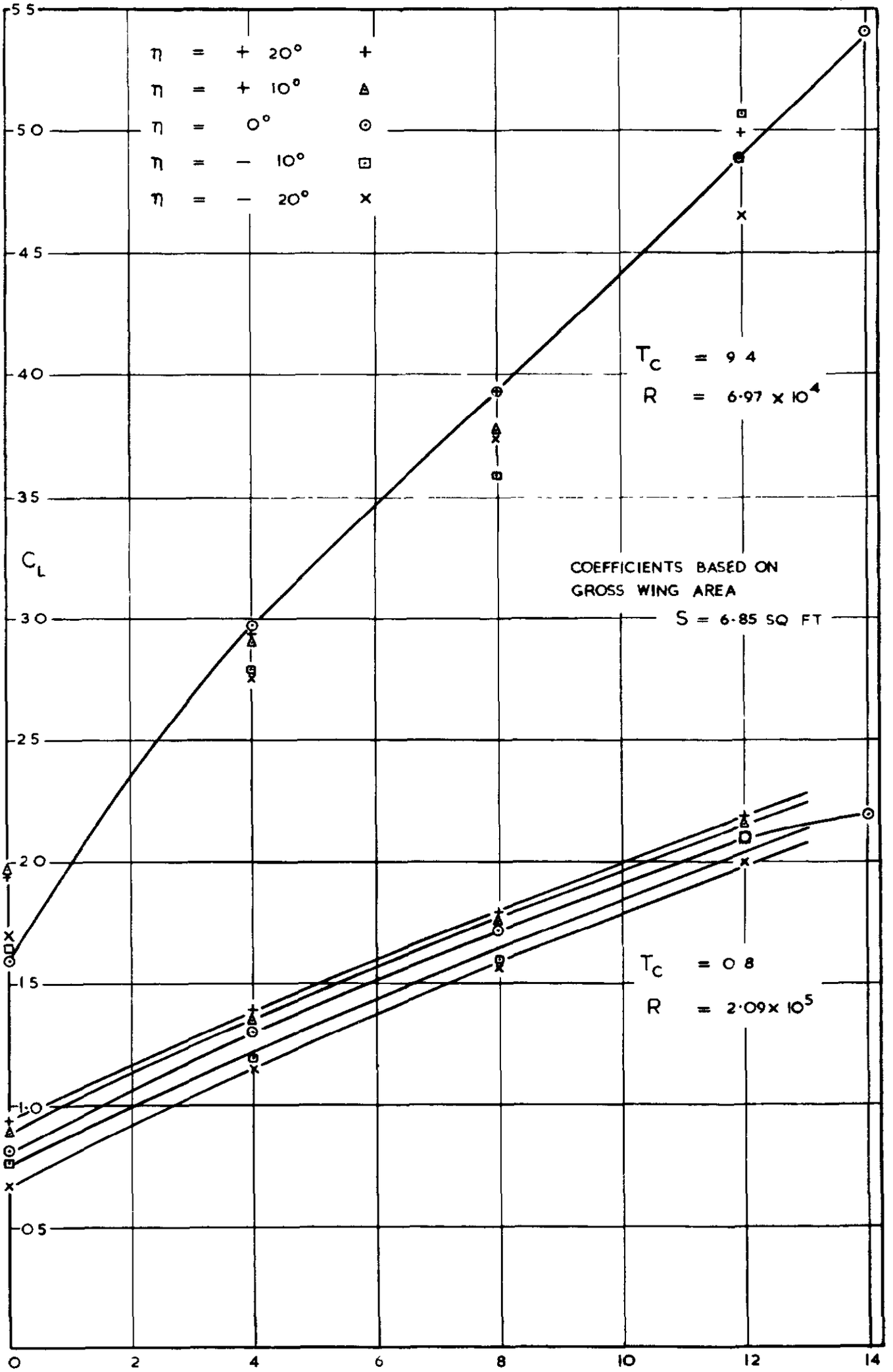

LIFT CURVES WITH TAKE-OFF POWER (1)

FIG. 4a. (2)

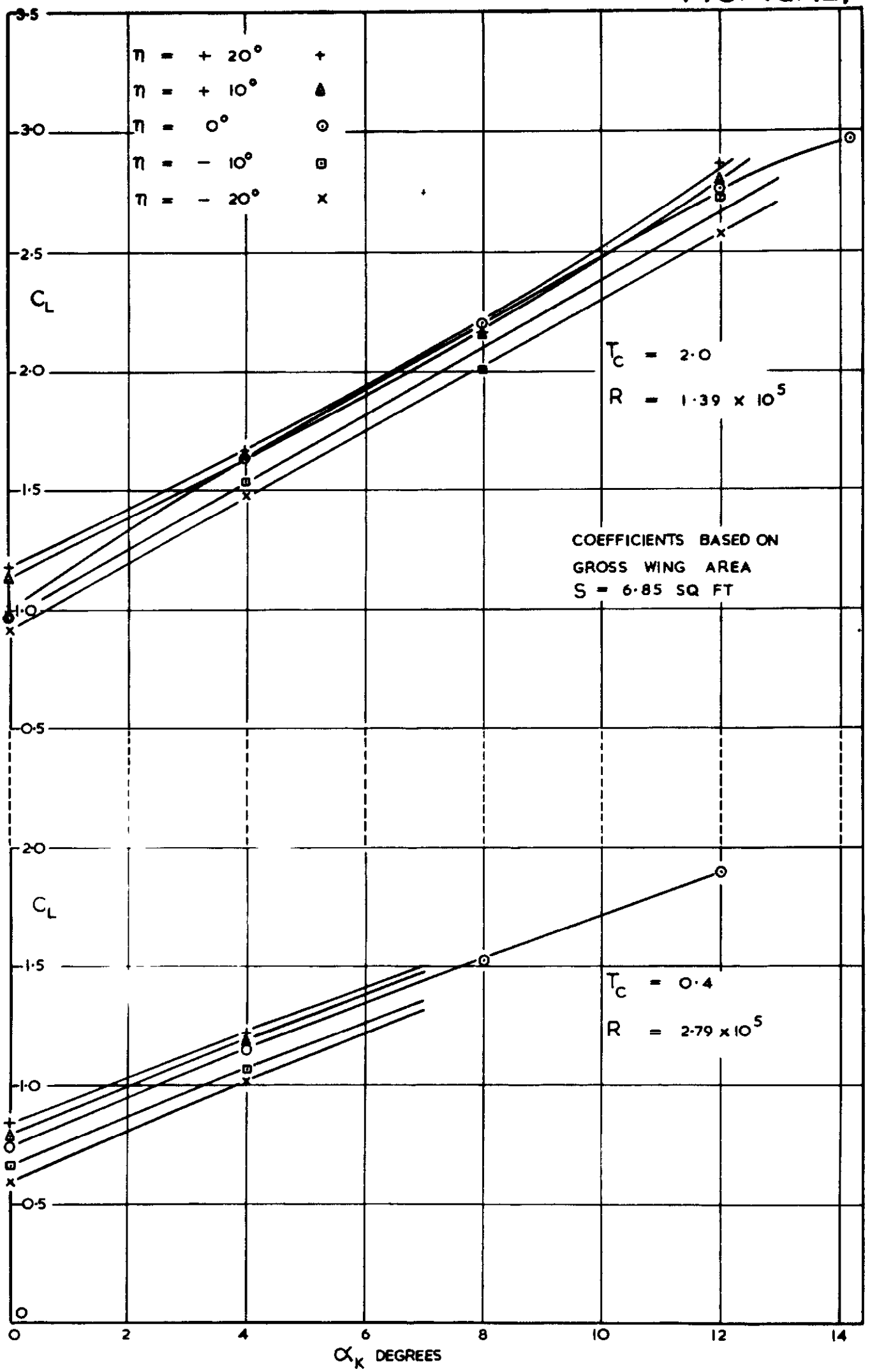

LIFT CURVES WITH TAKE-OFF POWER (2)

FIG. 4b.

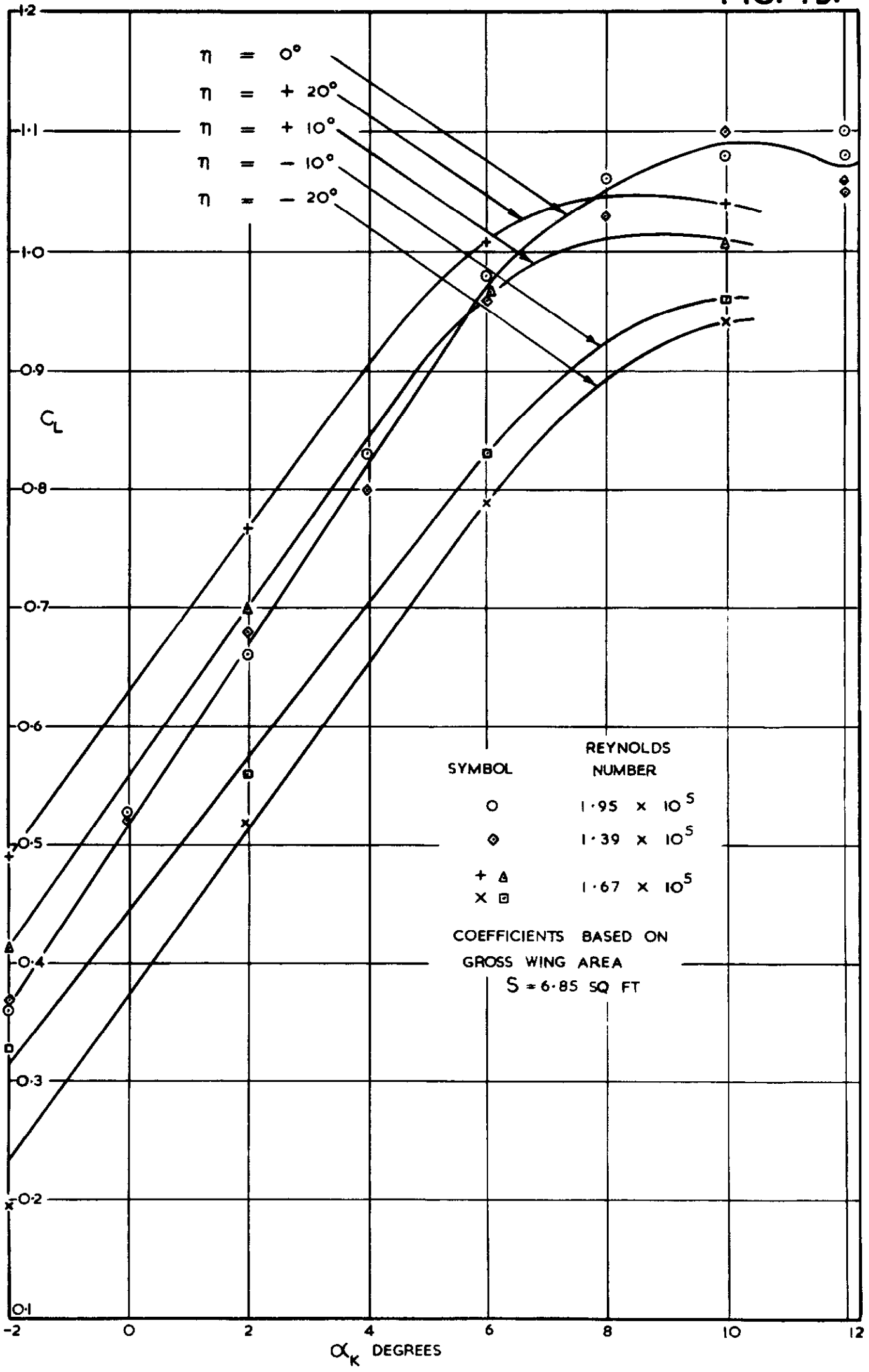

LIFT CURVES WITH PROPELLERS WINDMILLING

FIG. 4c.

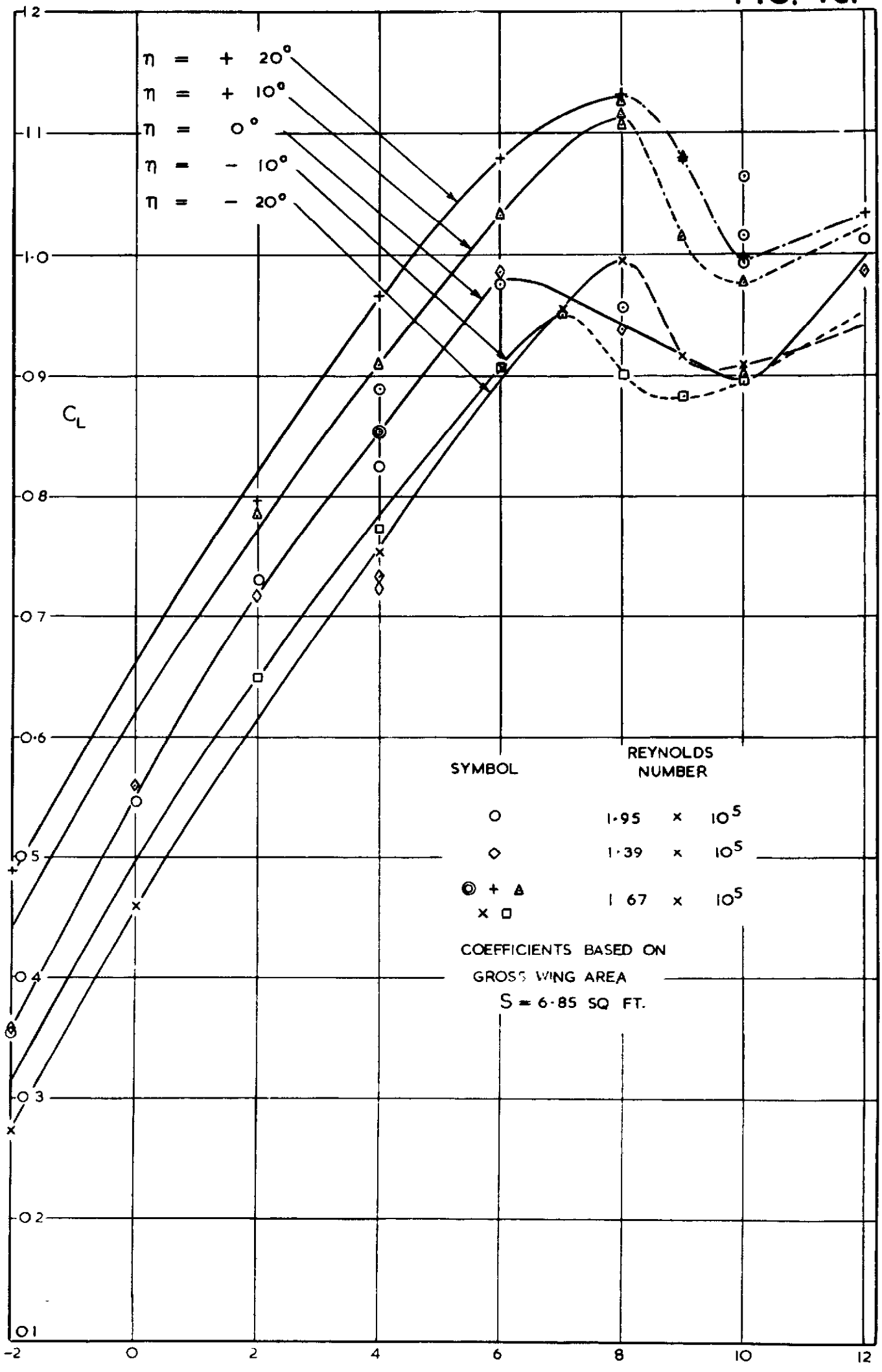

LIFT CURVES WITH FAIRINGS

FIG. 4d.

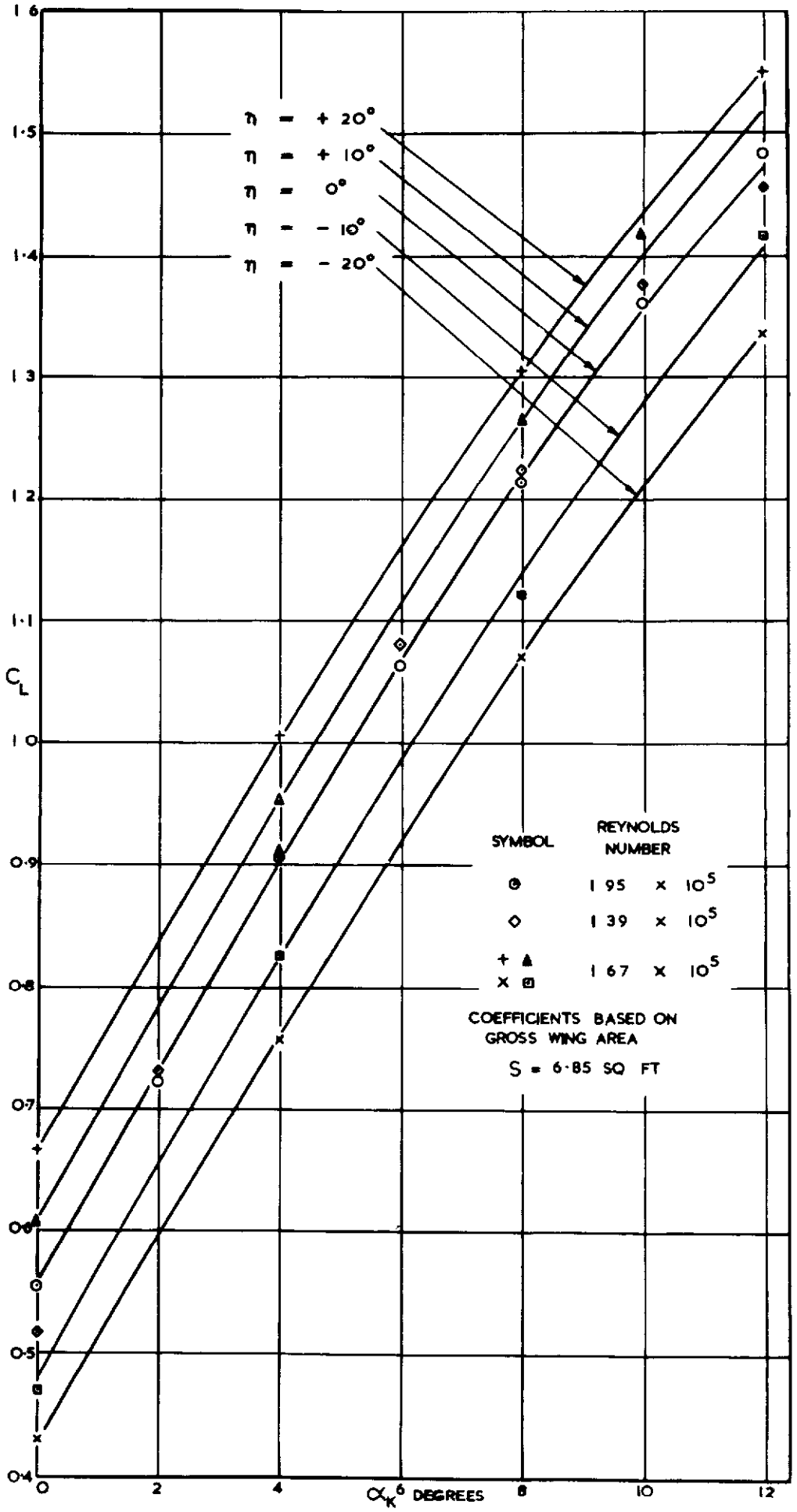

LIFT CURVES WITH FULL SPAN SLATS

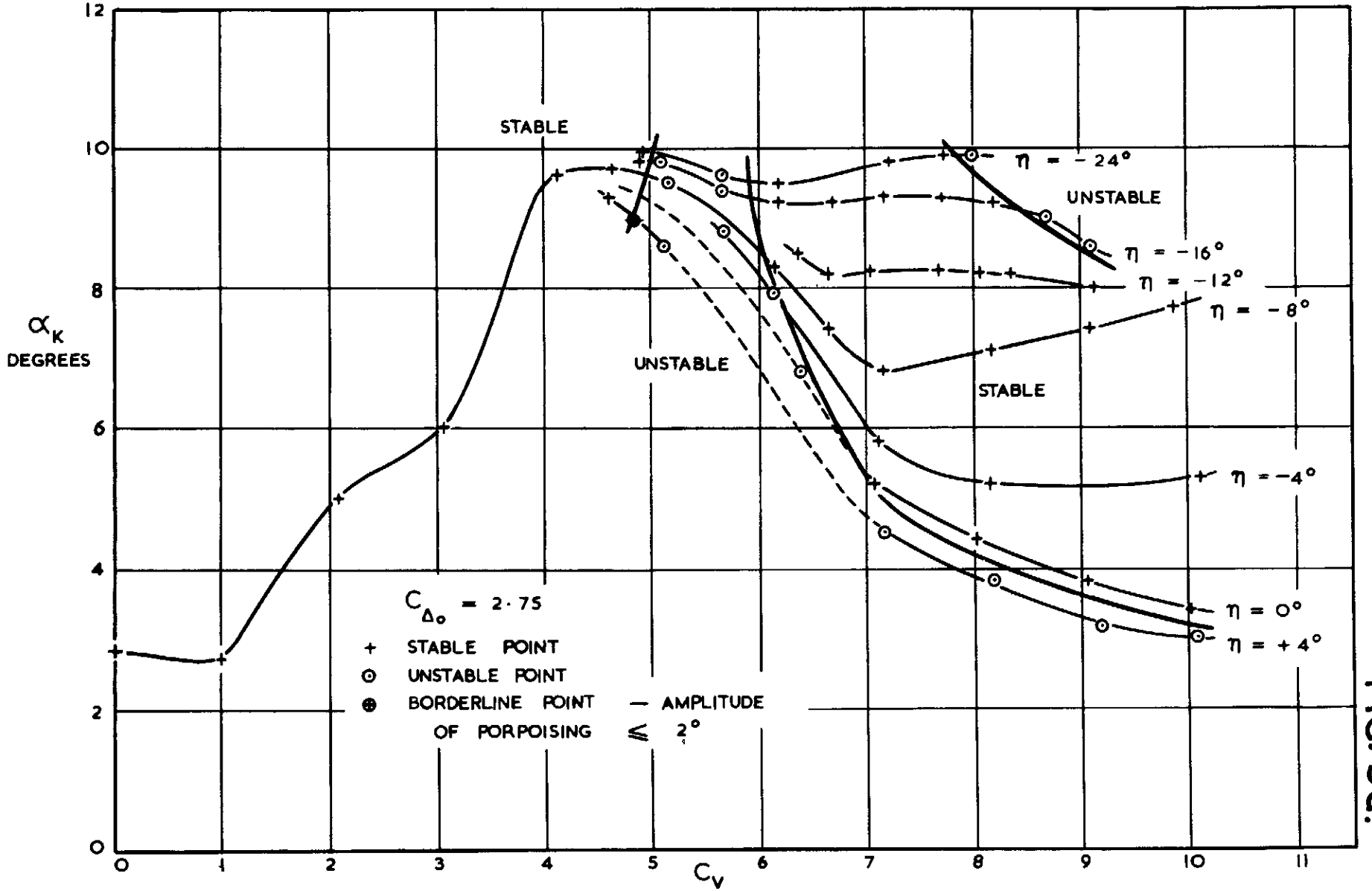

FIG. 5a.

MODEL A
LONGITUDINAL STABILITY WITHOUT DISTURBANCE WITH TAKE-OFF POWER

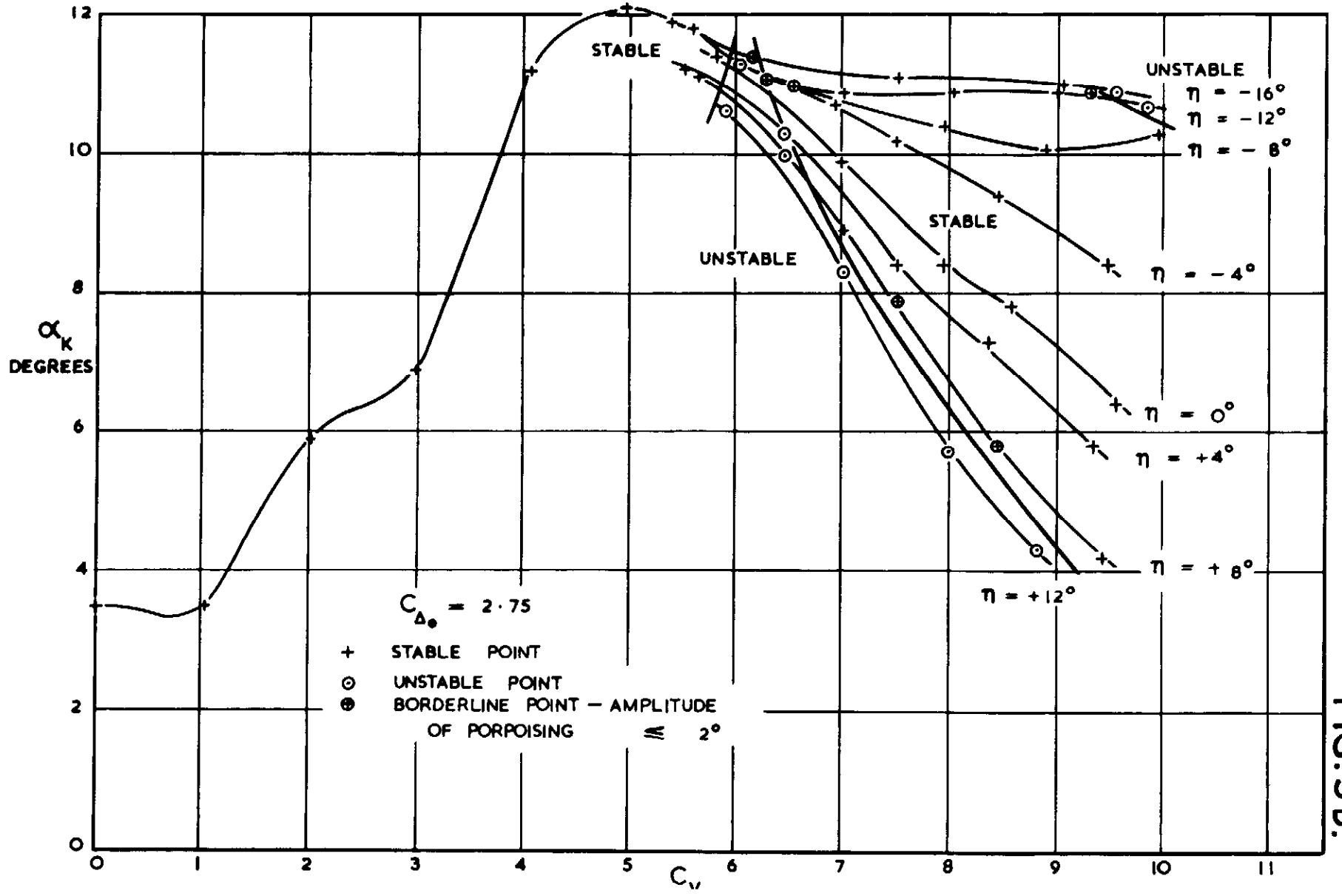

FIG. 5b.

MODEL A

LONGITUDINAL STABILITY WITHOUT DISTURBANCE WITH PROPELLERS WINDMILLING

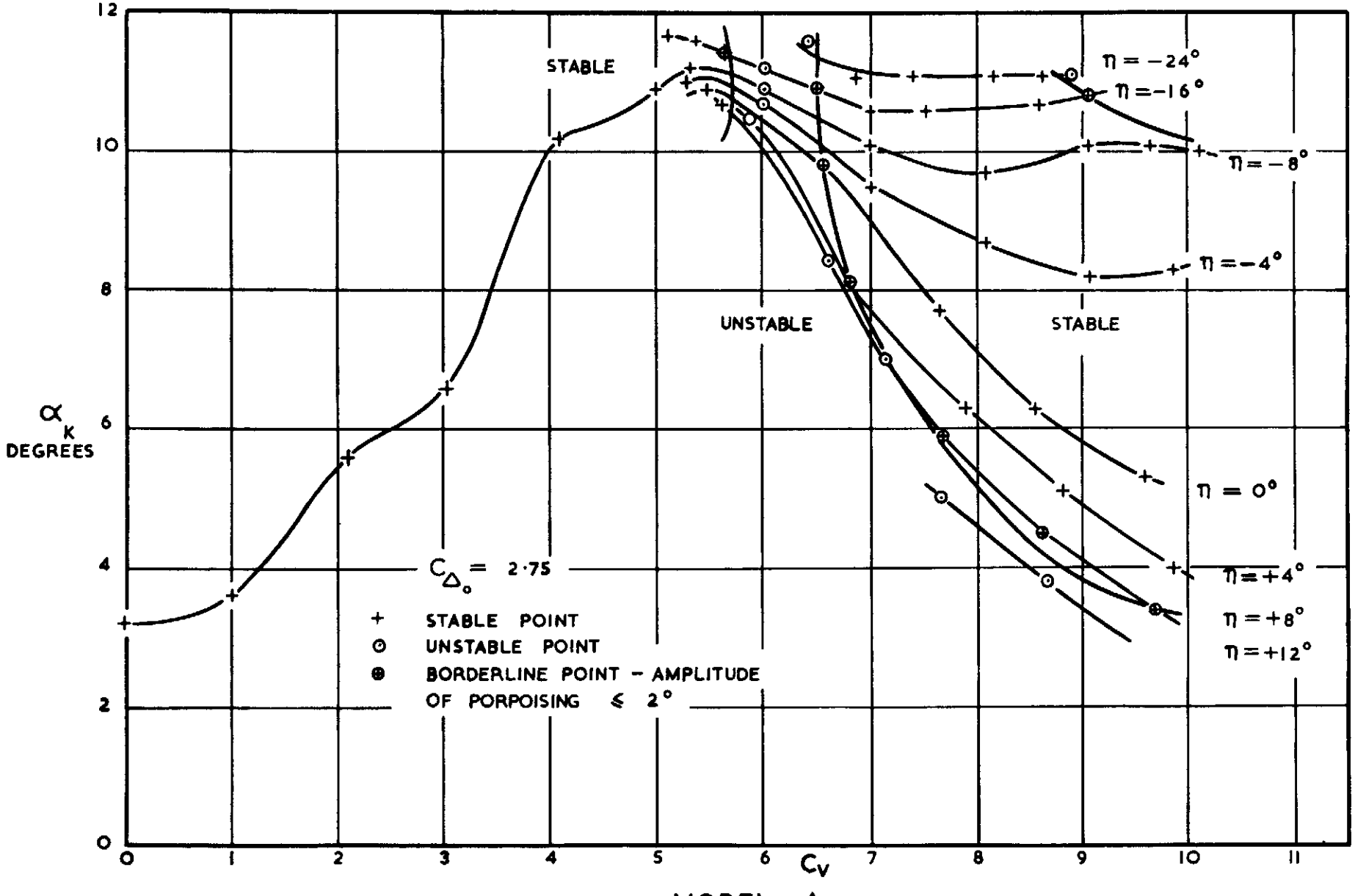

FIG. 5c.

MODEL A

LONGITUDINAL STABILITY WITHOUT DISTURBANCE WITH FAIRINGS

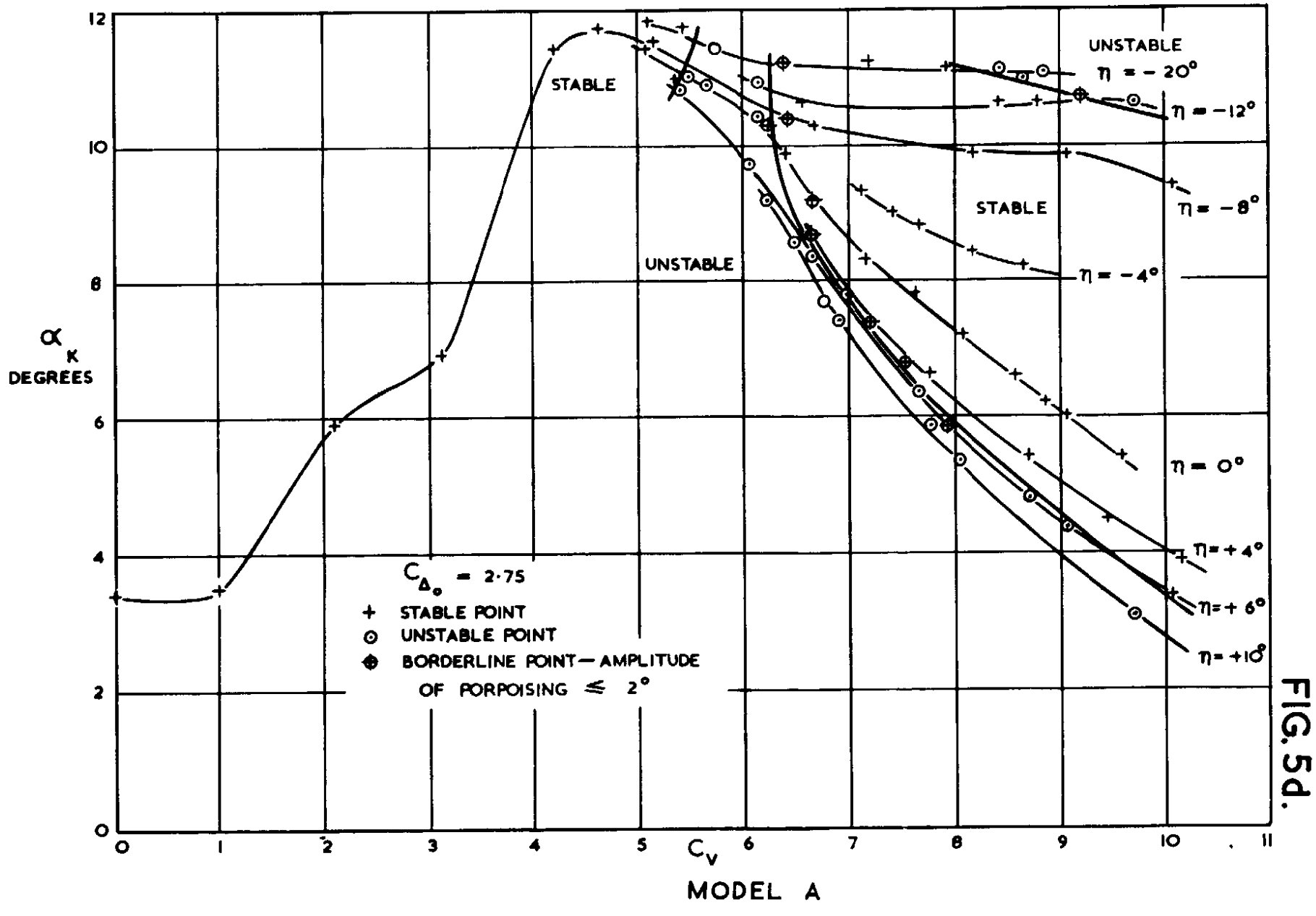

MODEL A

LONGITUDINAL STABILITY WITHOUT DISTURBANCE WITH FULL SPAN SLATS

FIG. 5d.

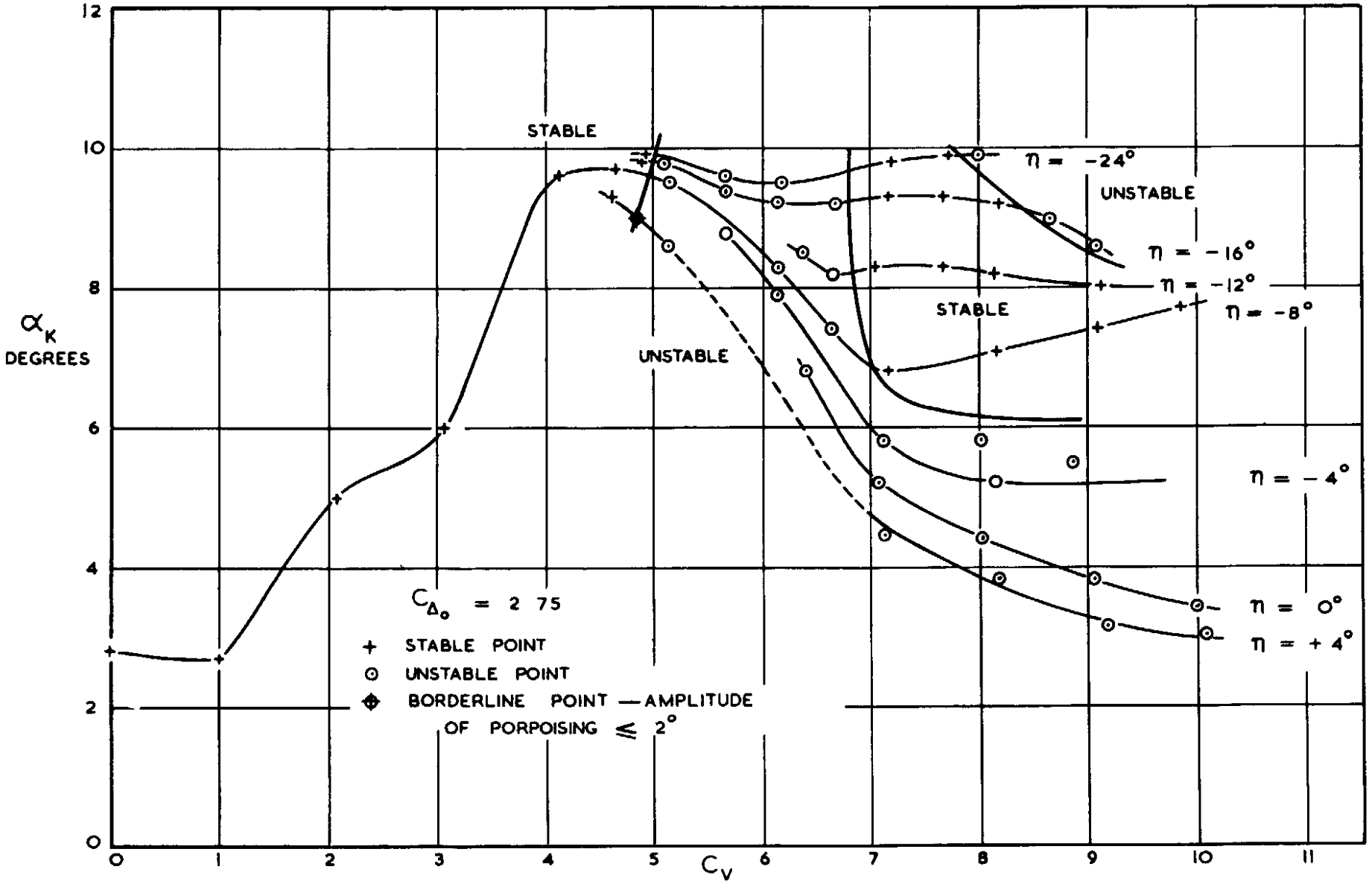

FIG. 6a.

MODEL A

LONGITUDINAL STABILITY WITH DISTURBANCE WITH TAKE-OFF POWER

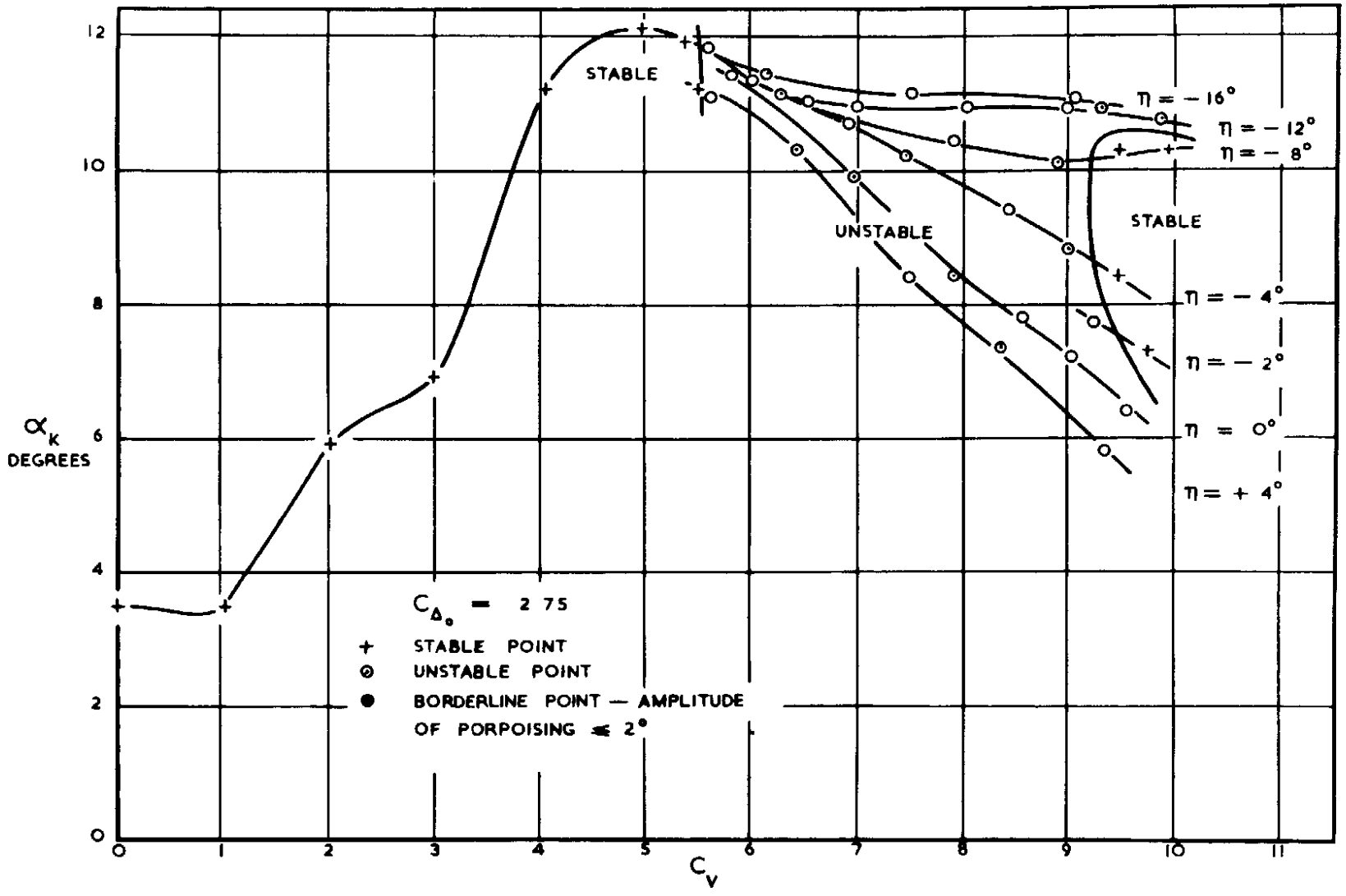

MODEL A

LONGITUDINAL STABILITY WITH DISTURBANCE WITH PROPELLERS WINDMILLING

FIG. 6b.

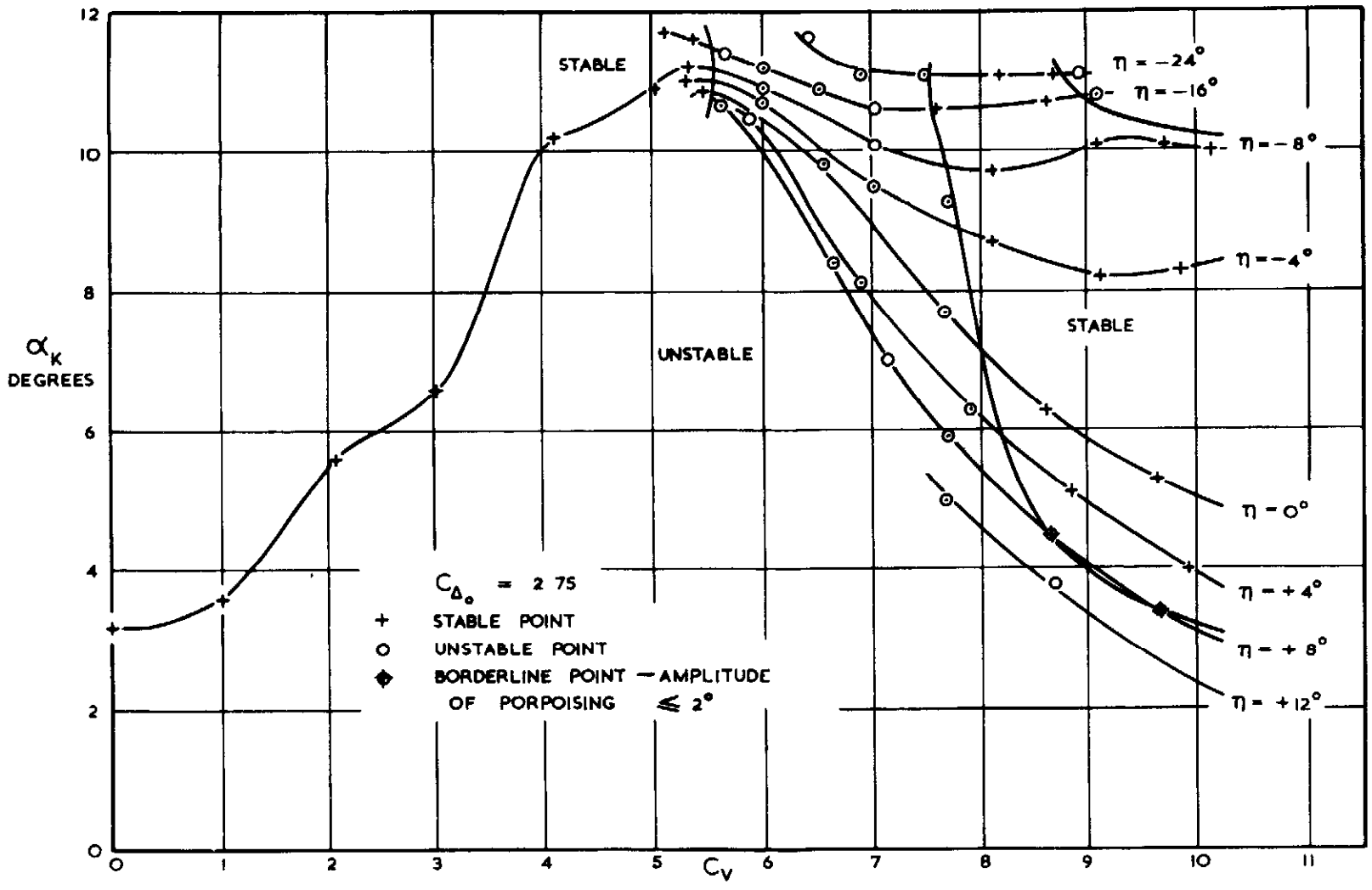

MODEL A

LONGITUDINAL STABILITY WITH DISTURBANCE (5° DISTURBANCE ONLY) WITH FAIRINGS

FIG. 6c.

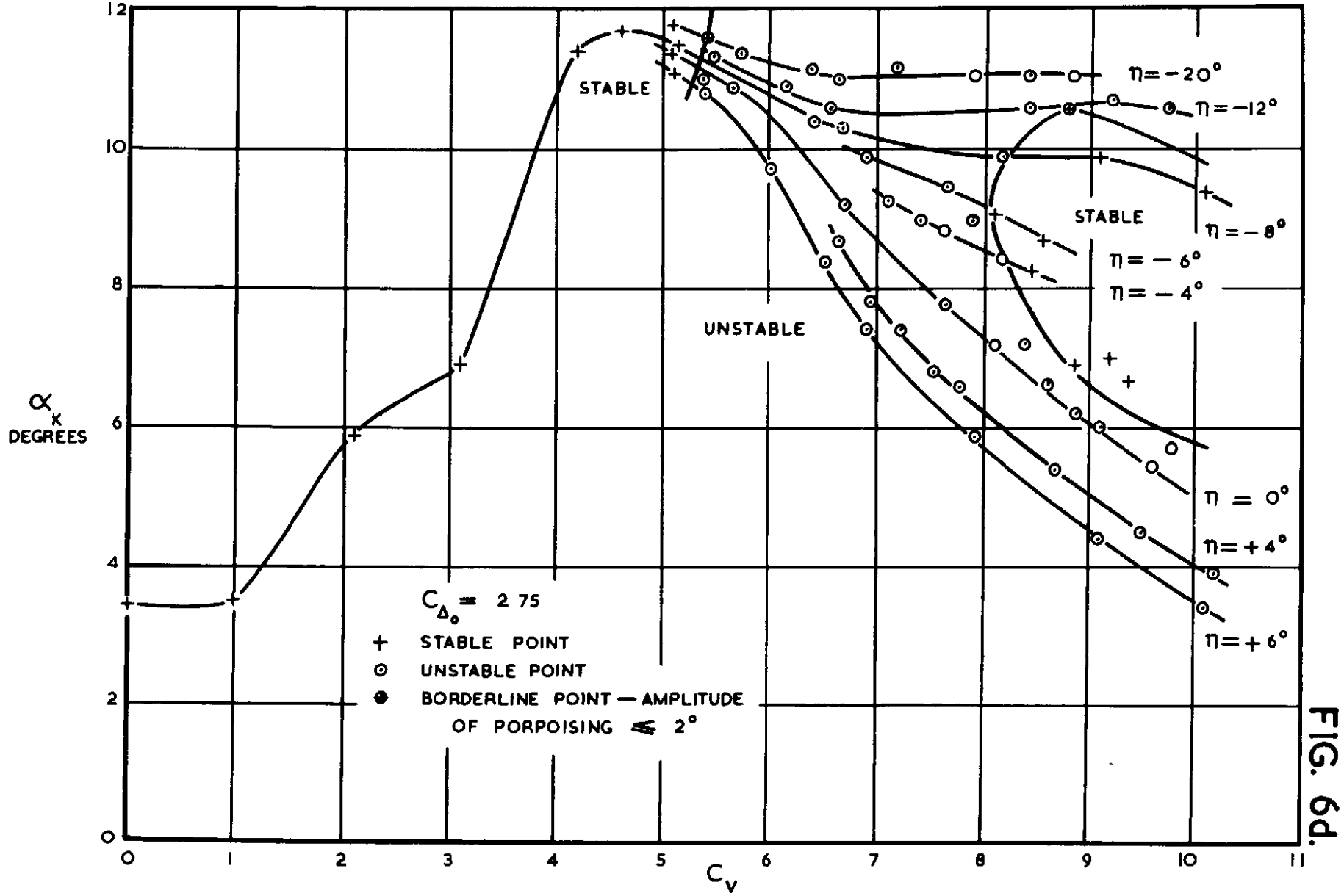

FIG. 6d.

MODEL A

LONGITUDINAL STABILITY WITH DISTURBANCE WITH FULL SPAN SLATS

FIG. 7.

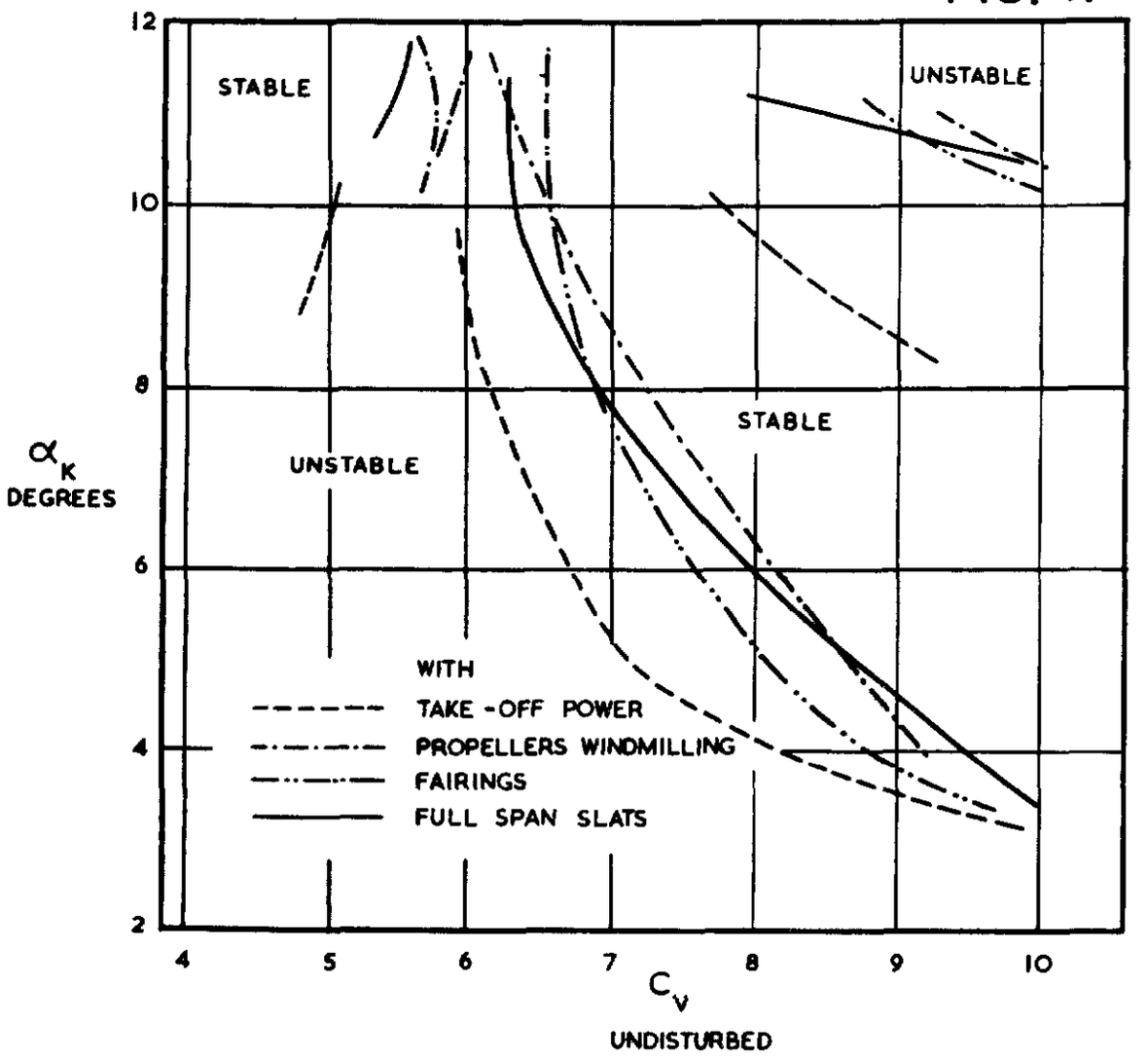

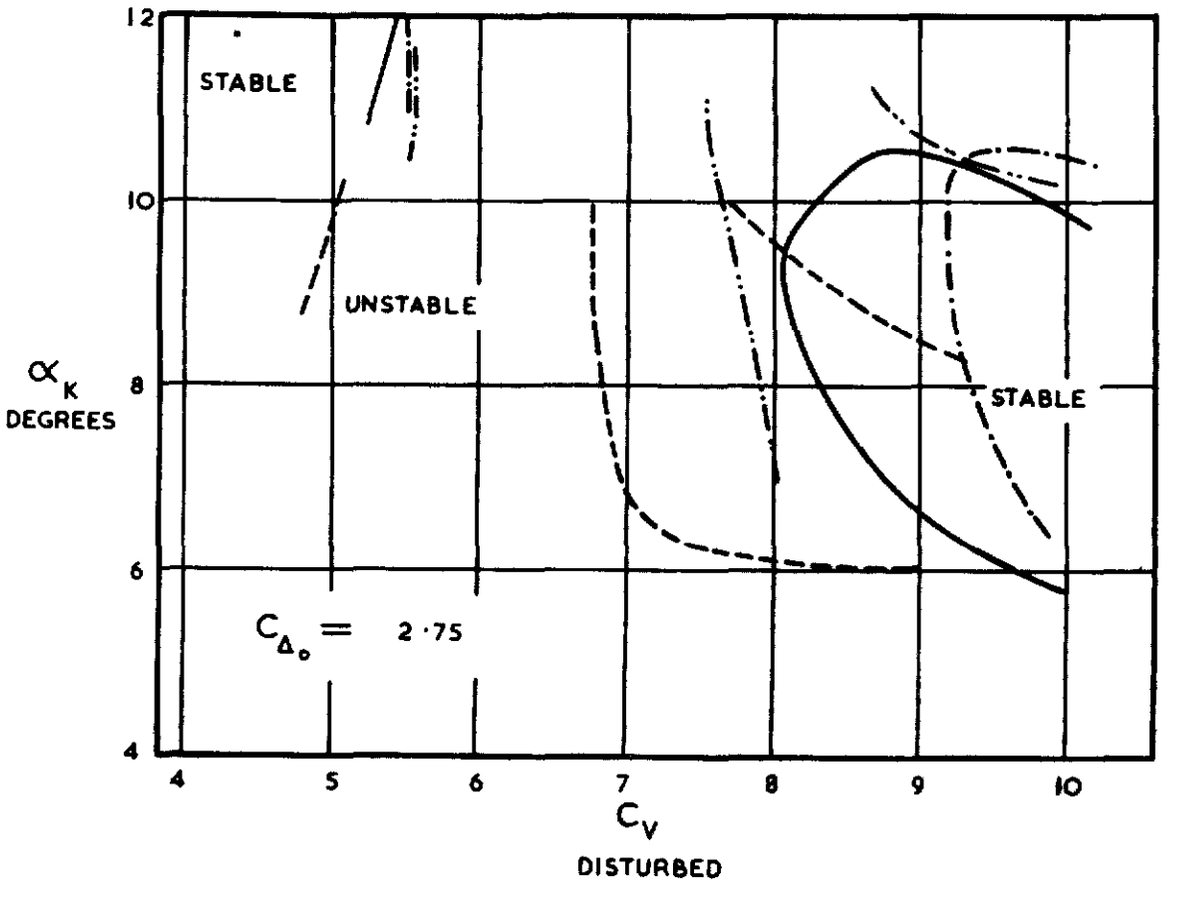

COMPARISON OF LONGITUDINAL STABILITY LIMITS ON A C_V BASE, MODEL A

FIG. 8.

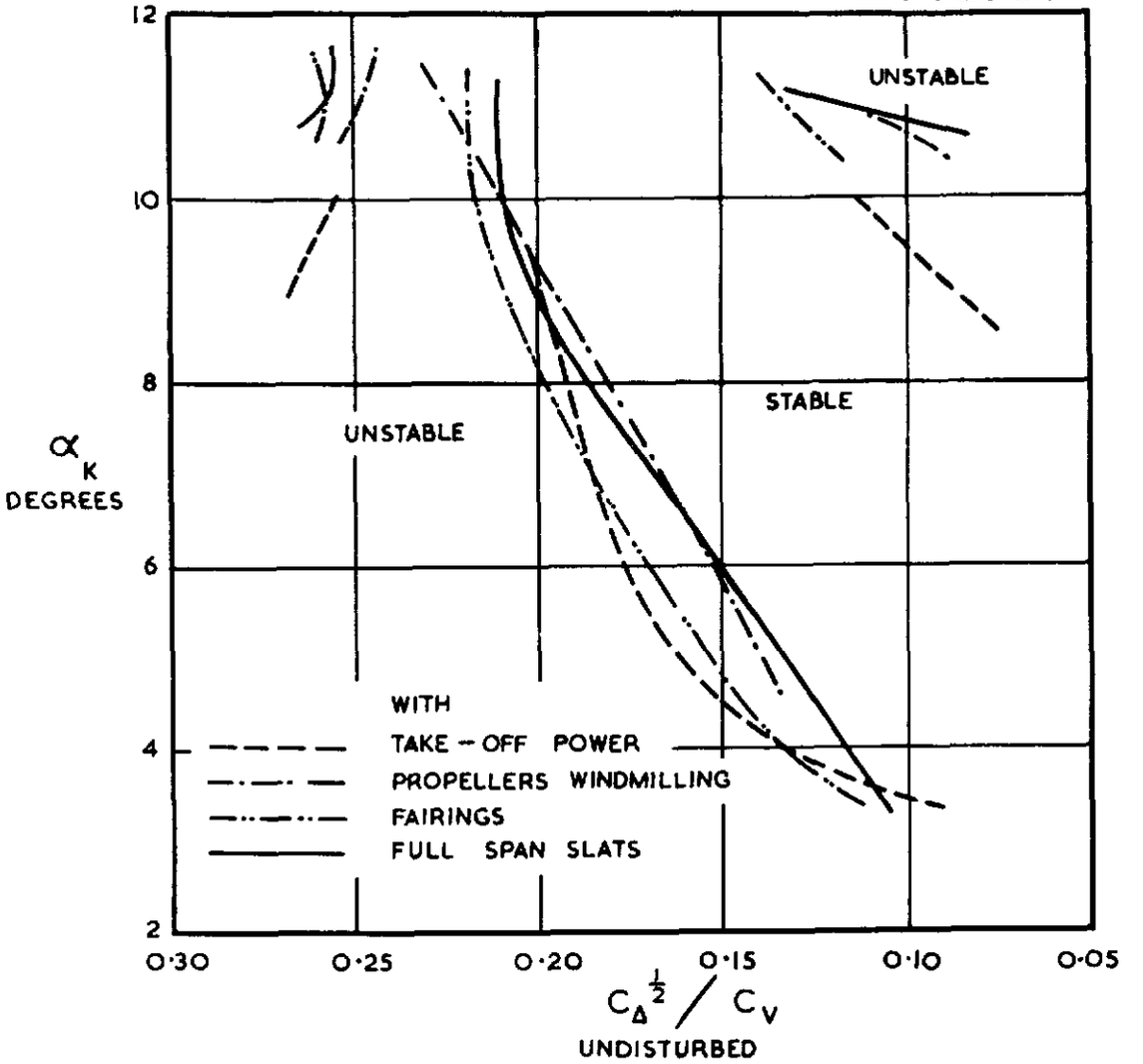

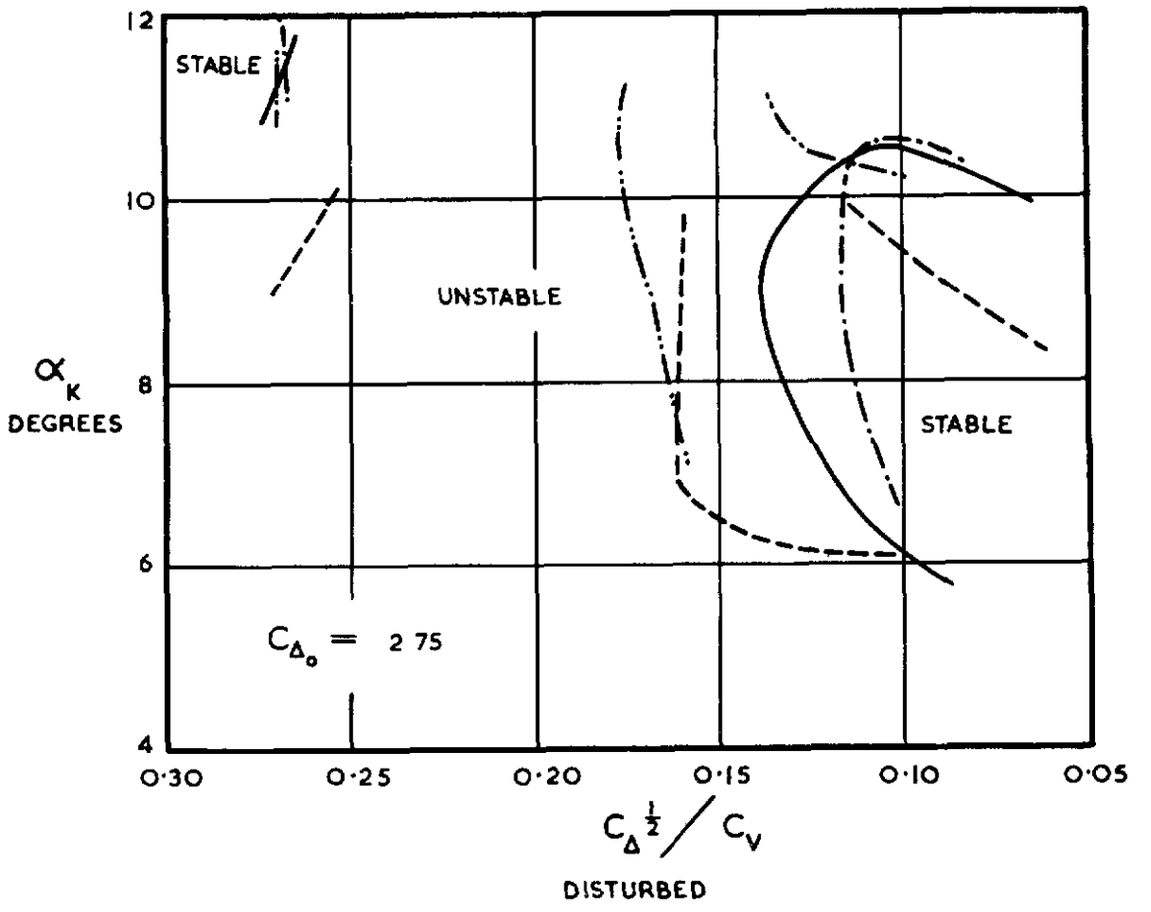

COMPARISON OF LONGITUDINAL STABILITY LIMITS ON A $C_\Delta^{\frac{1}{2}}/C_V$ BASE. MODEL A

FIG. 9.

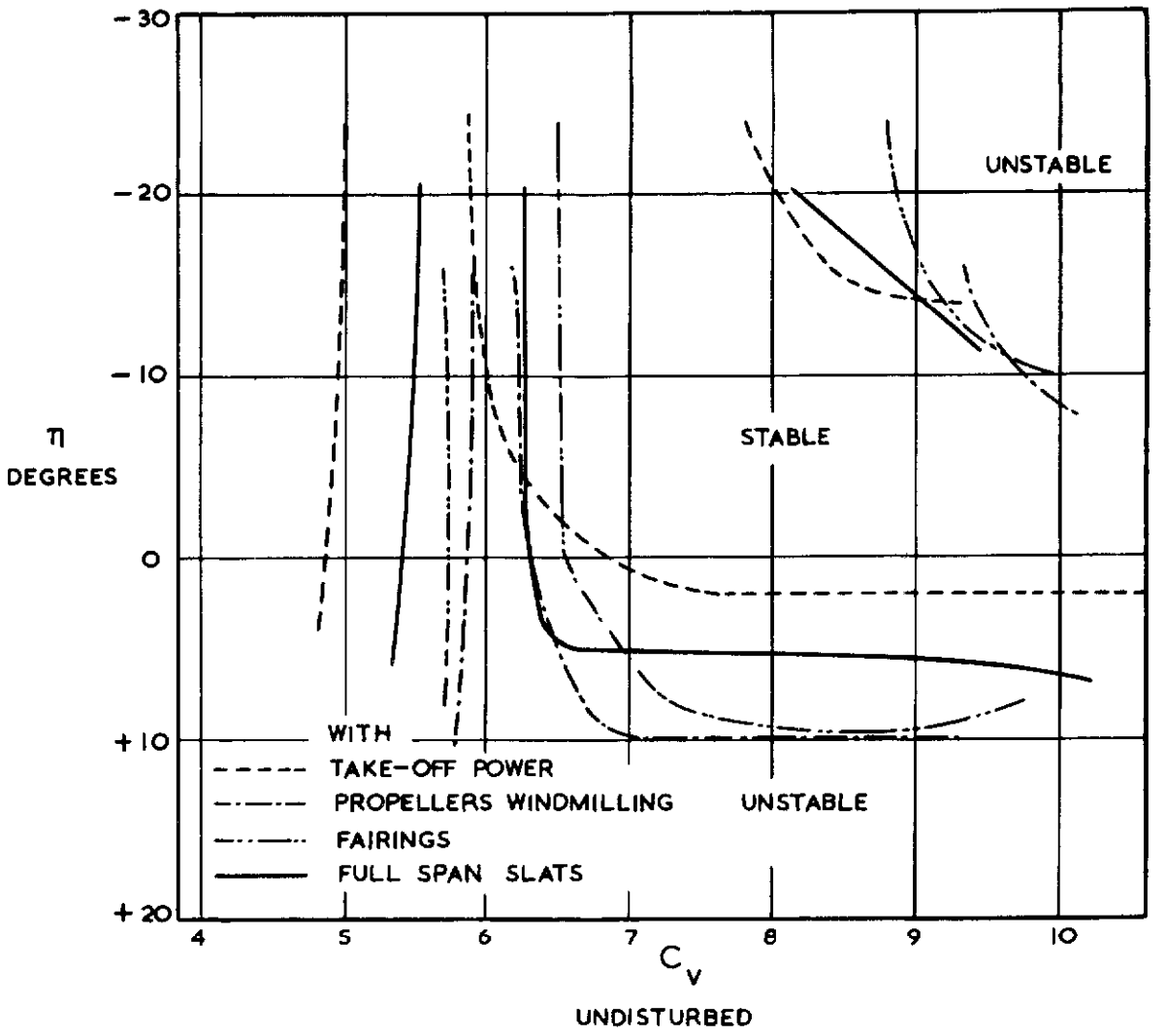

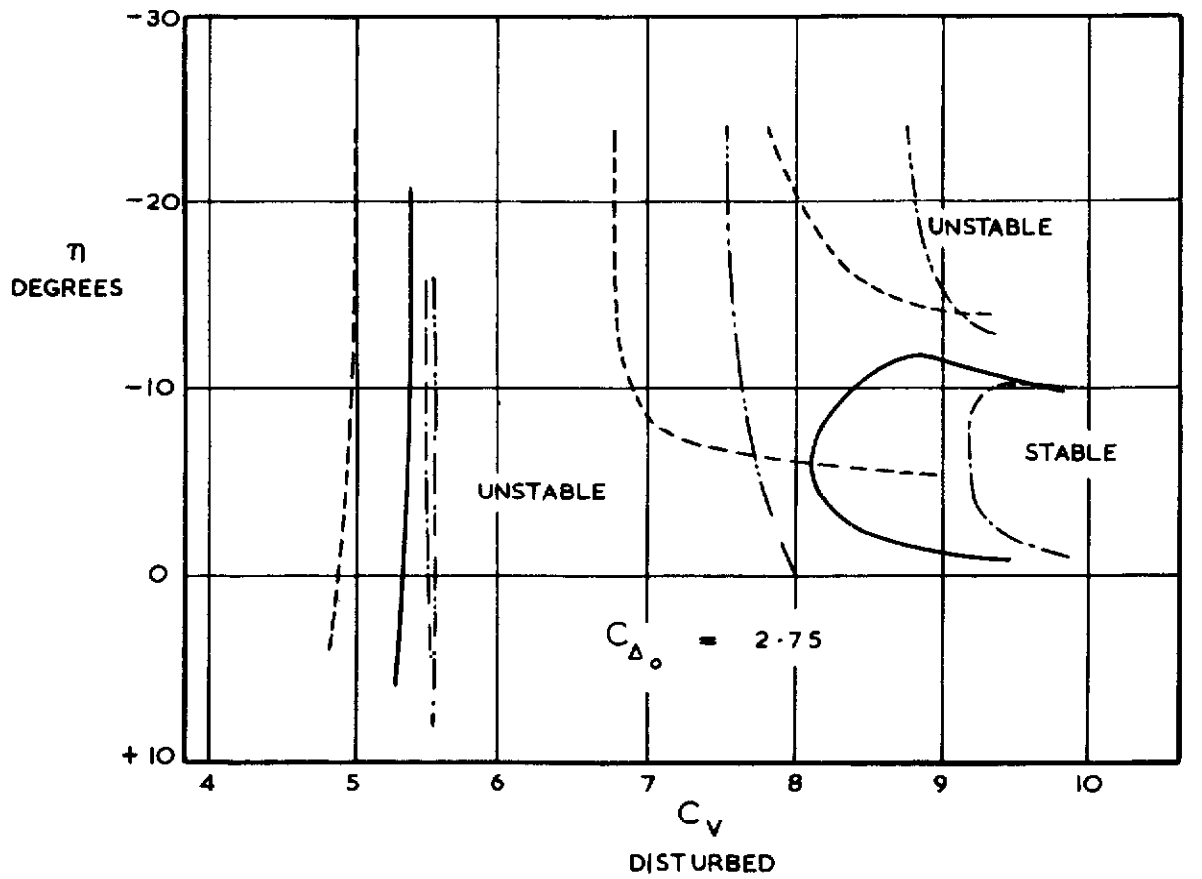

RELATION BETWEEN ELEVATOR SETTING AND STABILITY LIMITS

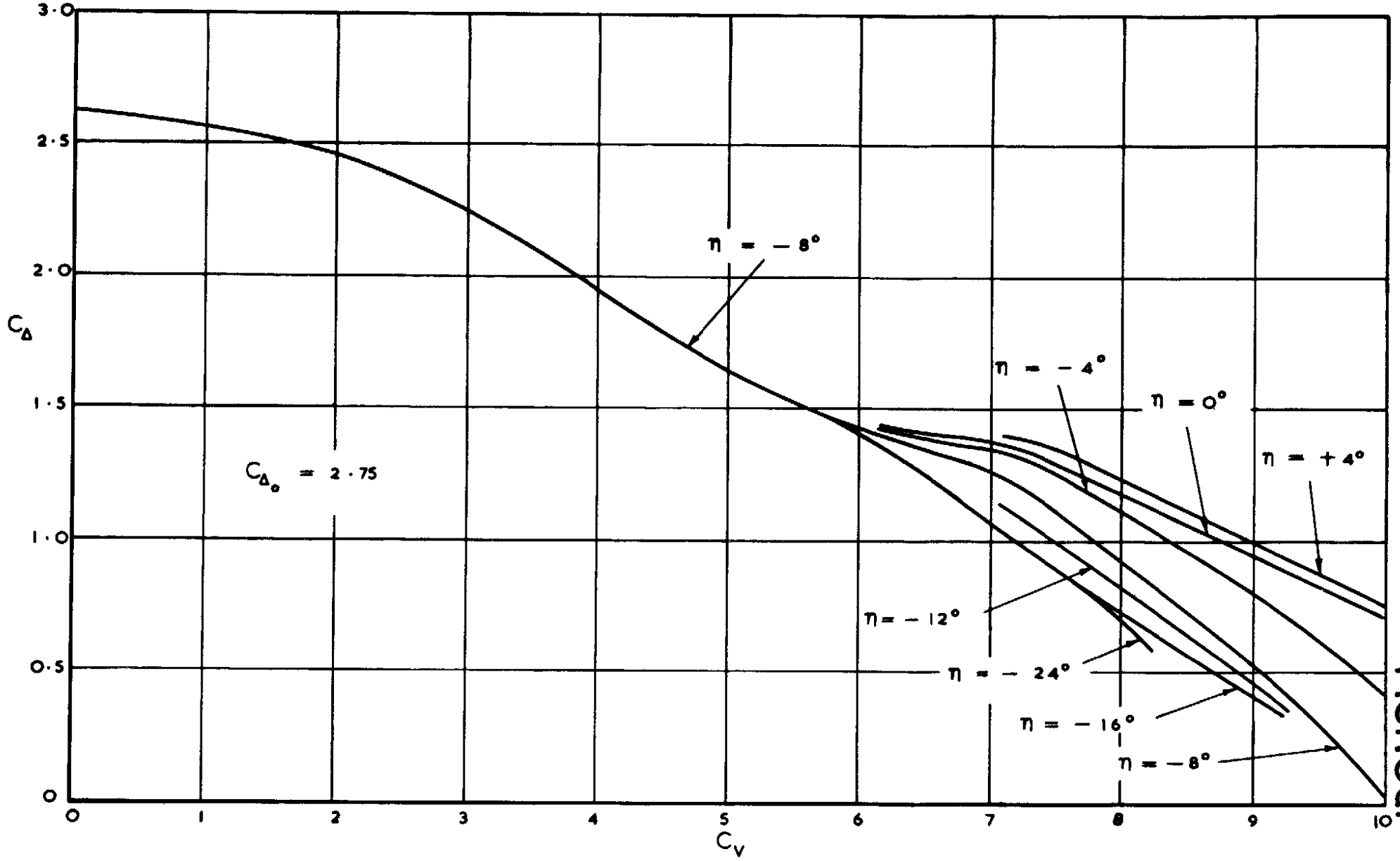

FIG. 10a.

MODEL A

LOAD COEFFICIENT CURVES WITH TAKE-OFF POWER

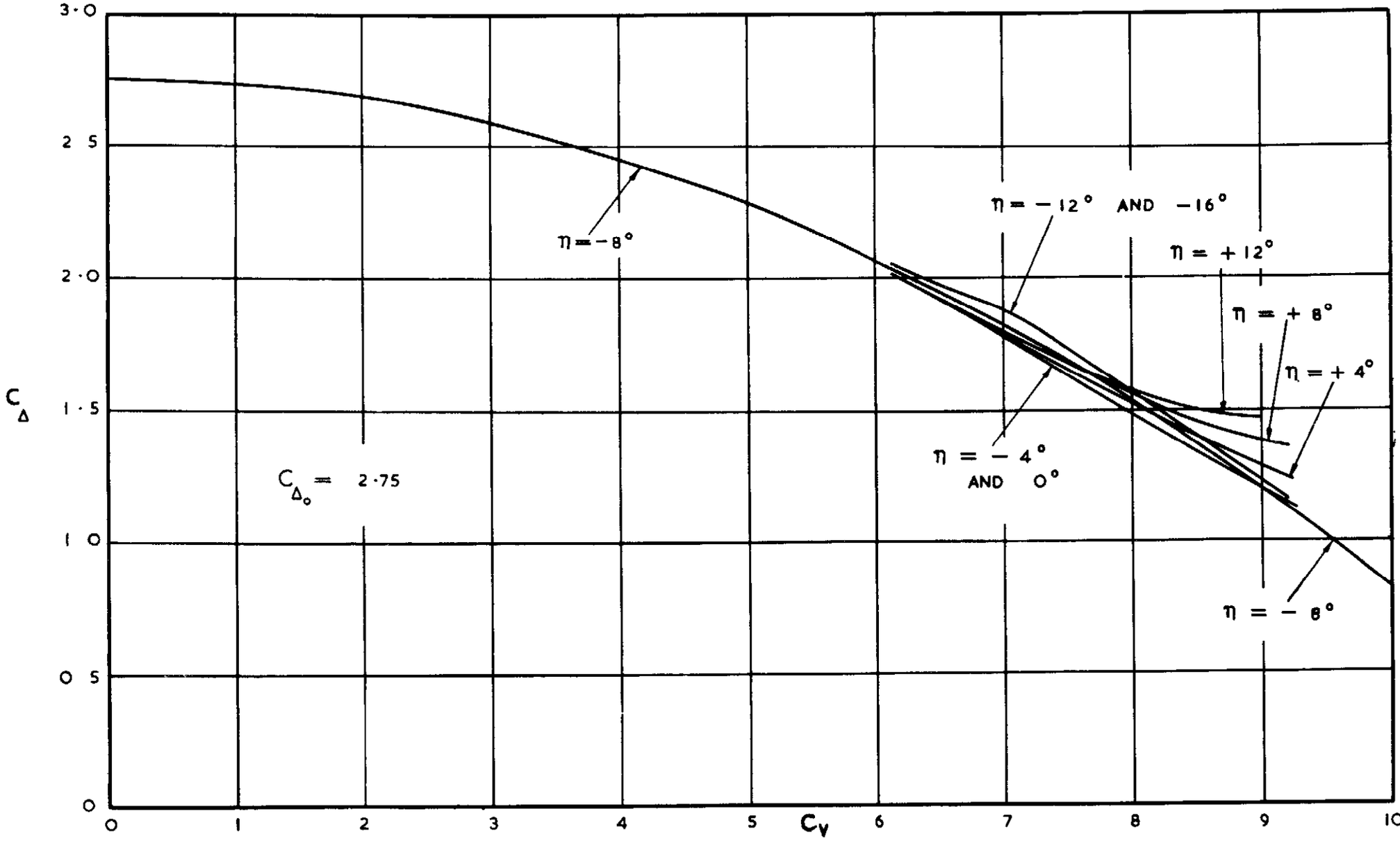

FIG. 10b.

MODEL A

LOAD COEFFICIENT CURVES WITH PROPELLERS WINDMILLING

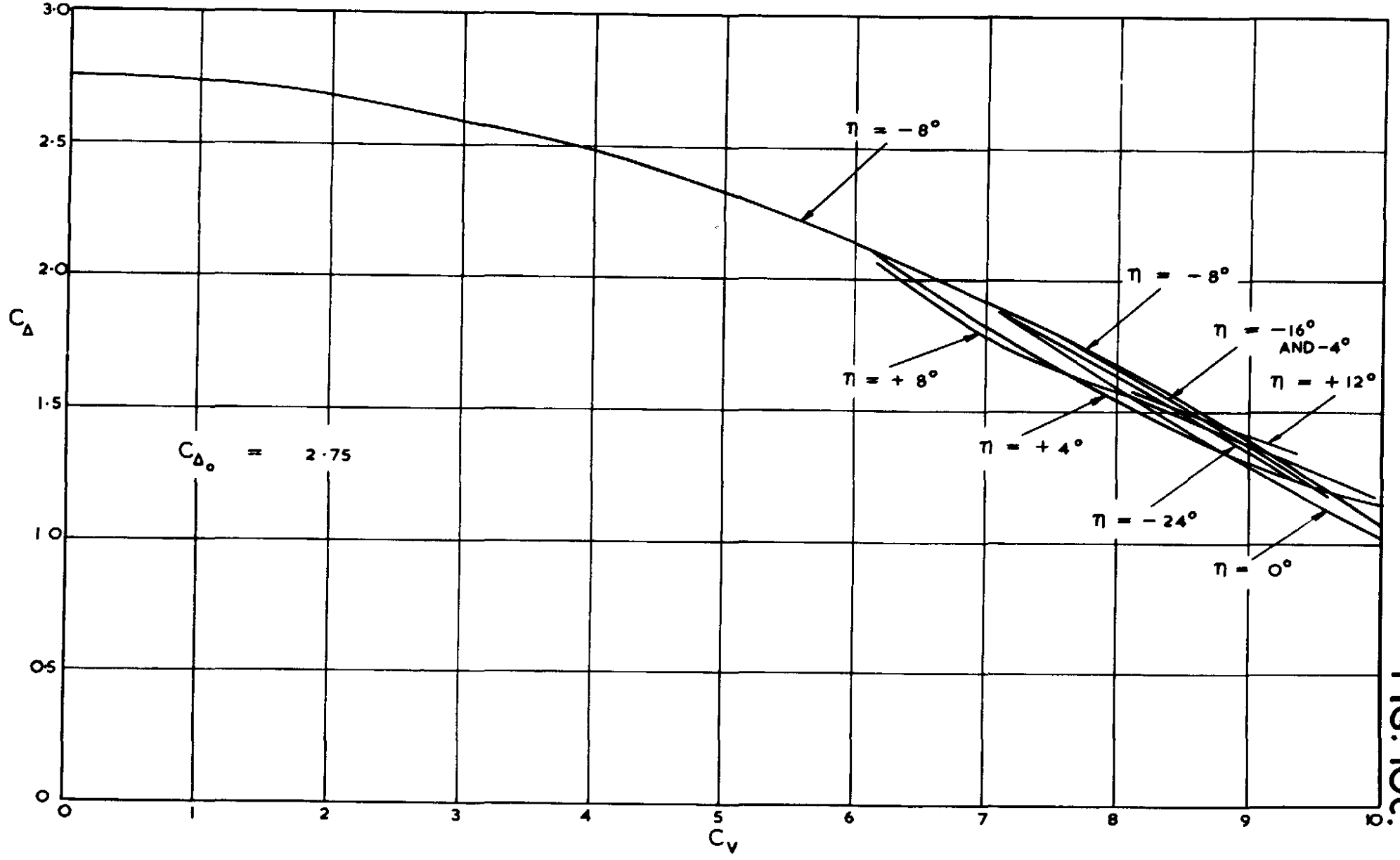

FIG. 10C.

MODEL A
LOAD COEFFICIENT CURVES WITH FAIRINGS

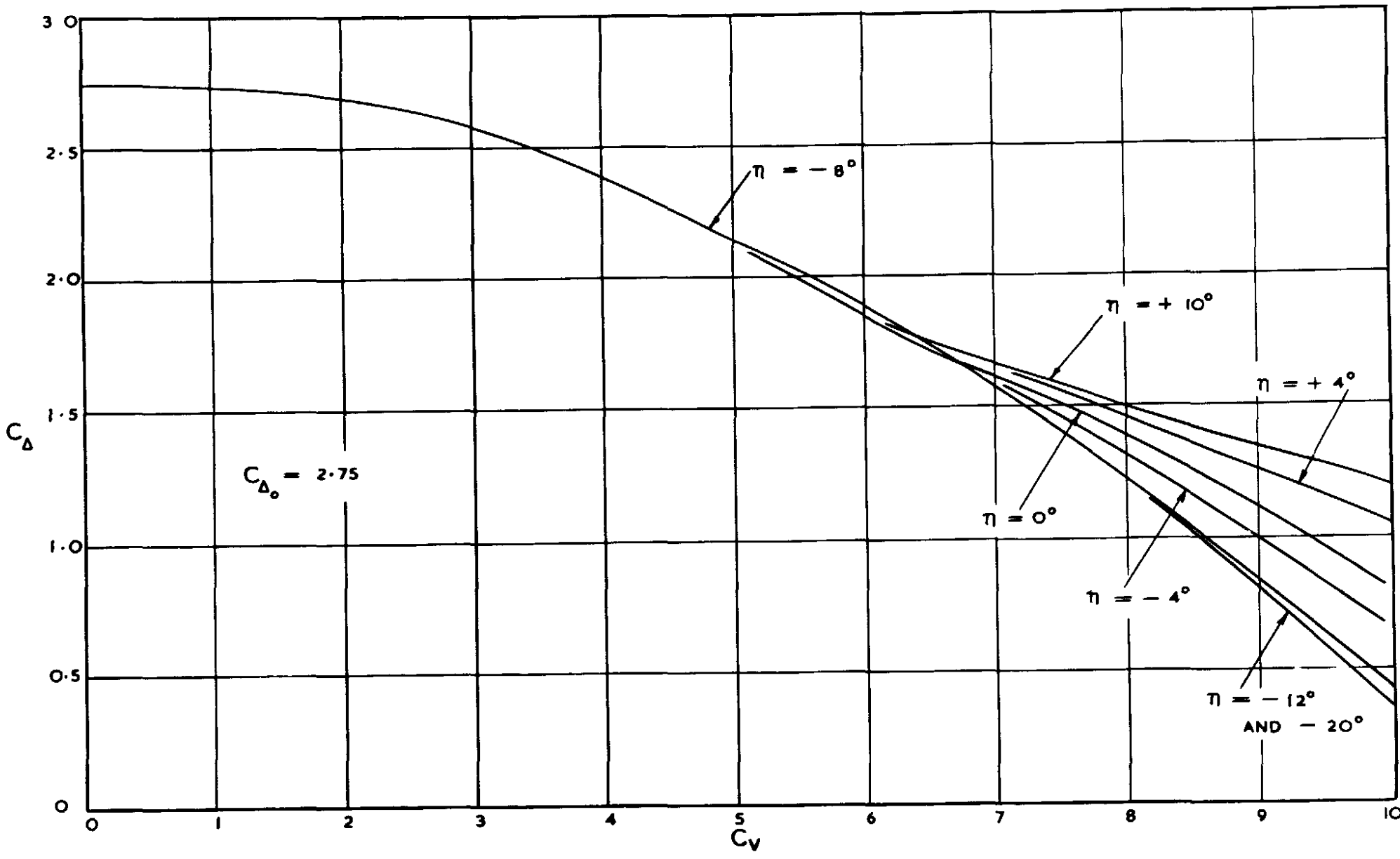

FIG. 10d.

MODEL A

LOAD COEFFICIENT CURVES WITH FULL SPAN SLATS

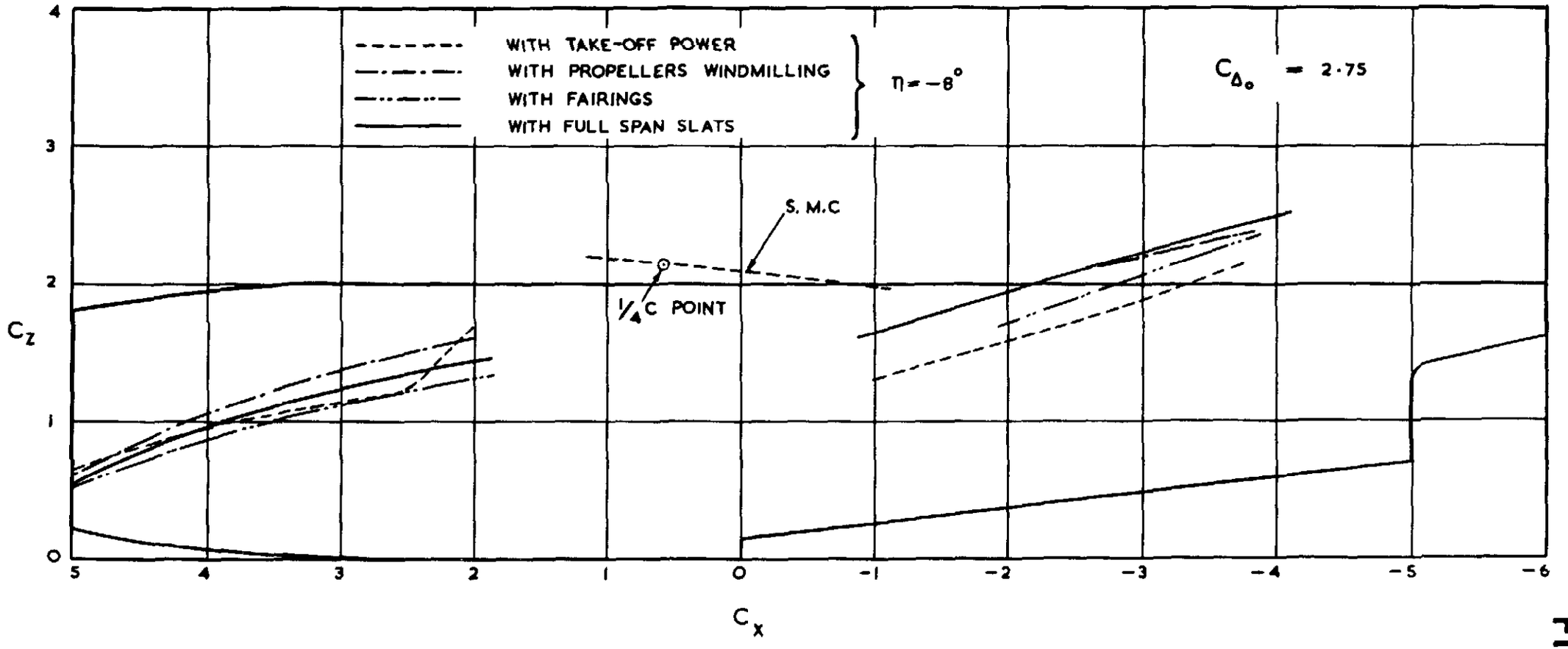

MODEL A

PROJECTIONS OF SPRAY ENVELOPES ON PLANE OF SYMMETRY OF MODEL

FIG. 13.

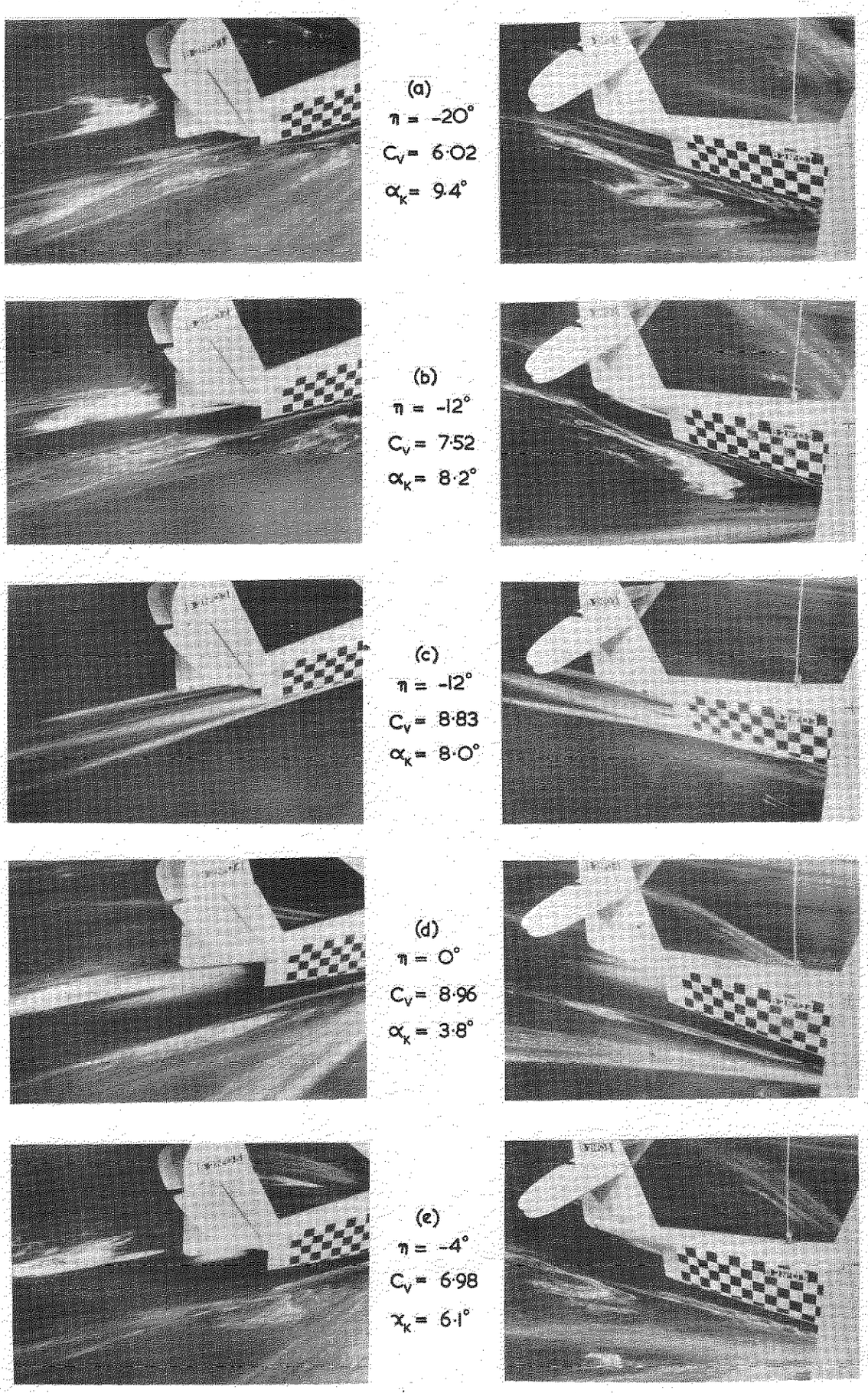

MODEL A

WAKE PHOTOGRAPHS WITH TAKE-OFF POWER

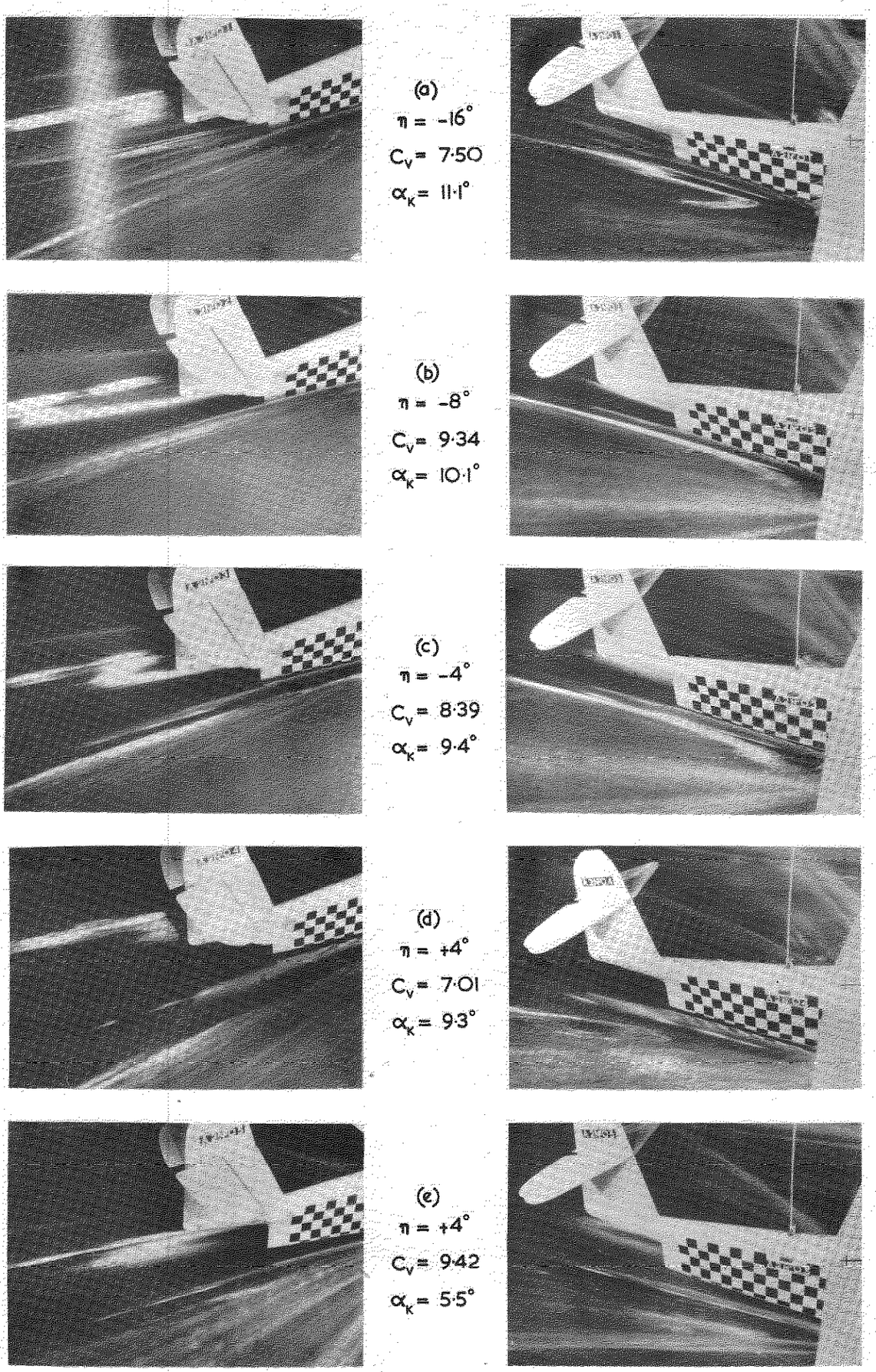

(a)
$\eta = -16°$
$C_v = 7.50$
$\alpha_K = 11.1°$

(b)
$\eta = -8°$
$C_v = 9.34$
$\alpha_K = 10.1°$

(c)
$\eta = -4°$
$C_v = 8.39$
$\alpha_K = 9.4°$

(d)
$\eta = +4°$
$C_v = 7.01$
$\alpha_K = 9.3°$

(e)
$\eta = +4°$
$C_v = 9.42$
$\alpha_K = 5.5°$

MODEL A

WAKE PHOTOGRAPHS WITH PROPELLERS WINDMILLING

(a)
$\eta = -8°$
$C_v = 1{\cdot}00$
$\alpha_k = 2{\cdot}7°$

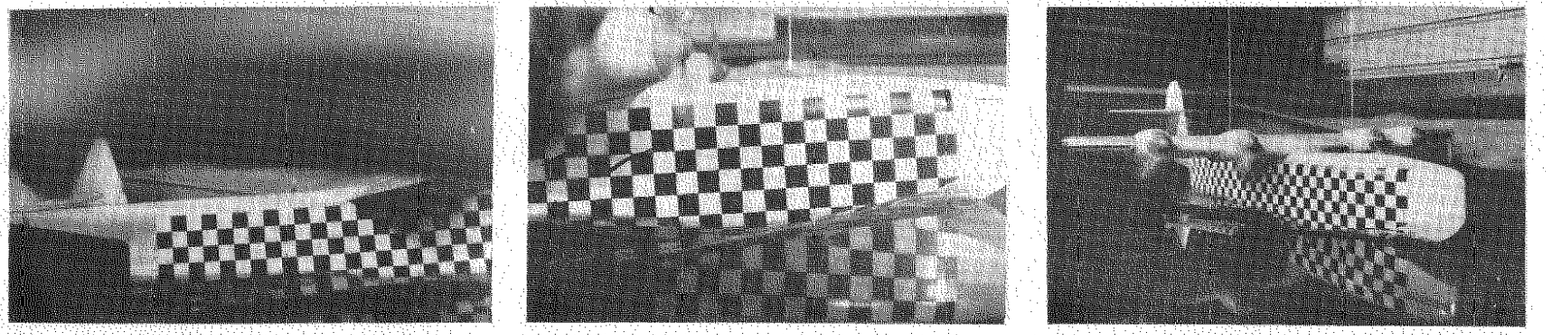

(b)
$\eta = -8°$
$C_v = 2{\cdot}07$
$\alpha_k = 5{\cdot}0°$

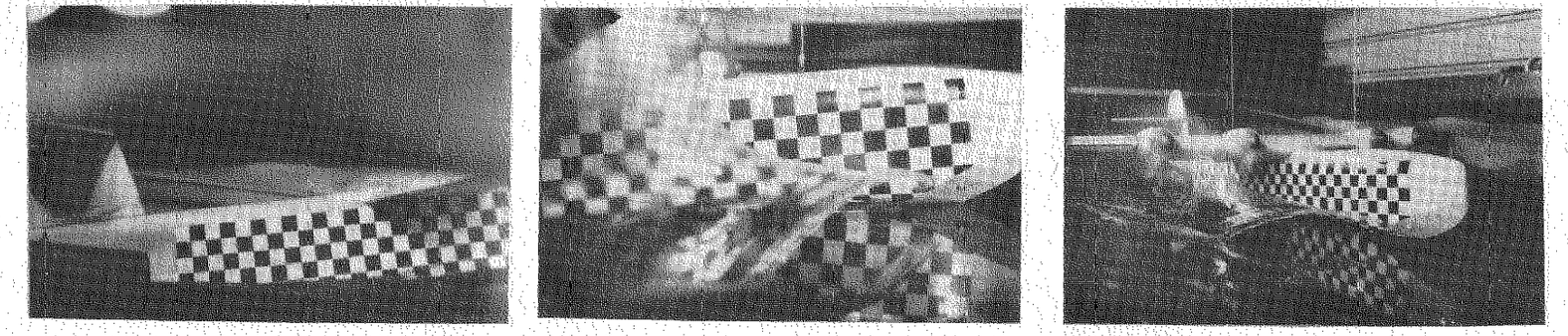

(c)
$\eta = -8°$
$C_v = 3{\cdot}10$
$\alpha_k = 6{\cdot}0°$

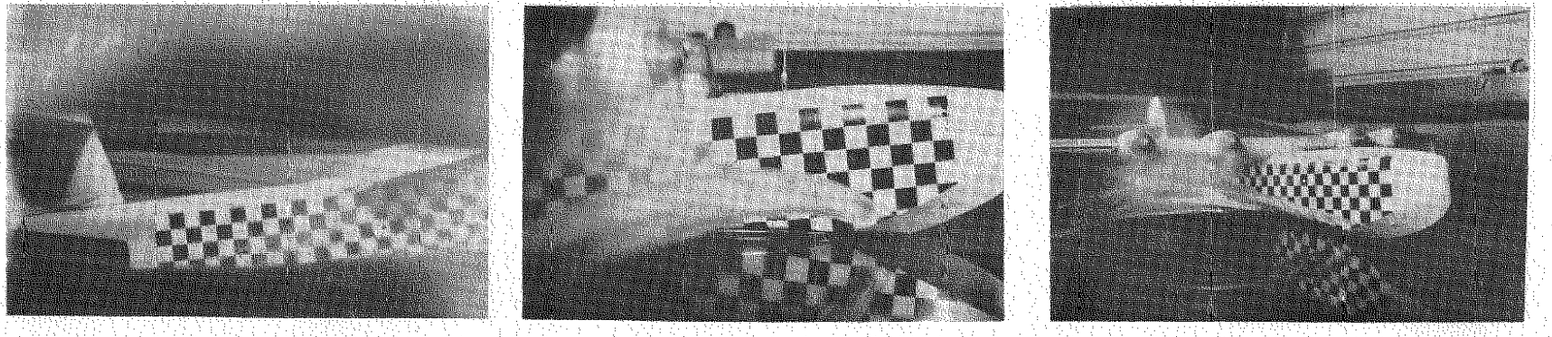

MODEL A

SPRAY PHOTOGRAPHS WITH TAKE-OFF POWER (1)

FIG. 12a (1)

(a)
$\eta = -8°$
$C_v = 4{\cdot}17$
$\alpha_k = 9{\cdot}6°$

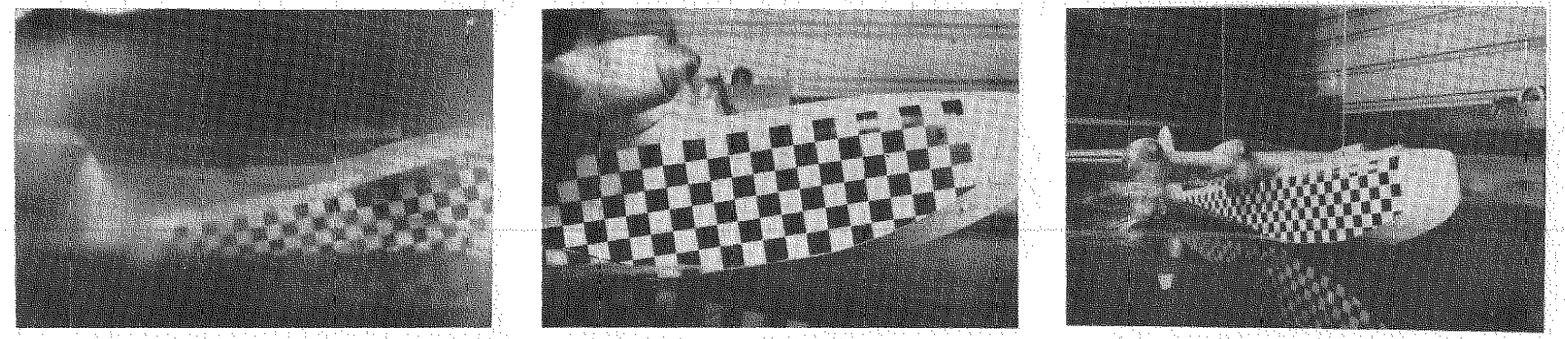

(b)
$\eta = -8°$
$C_v = 6{\cdot}14$
$\alpha_k = 8{\cdot}3°$

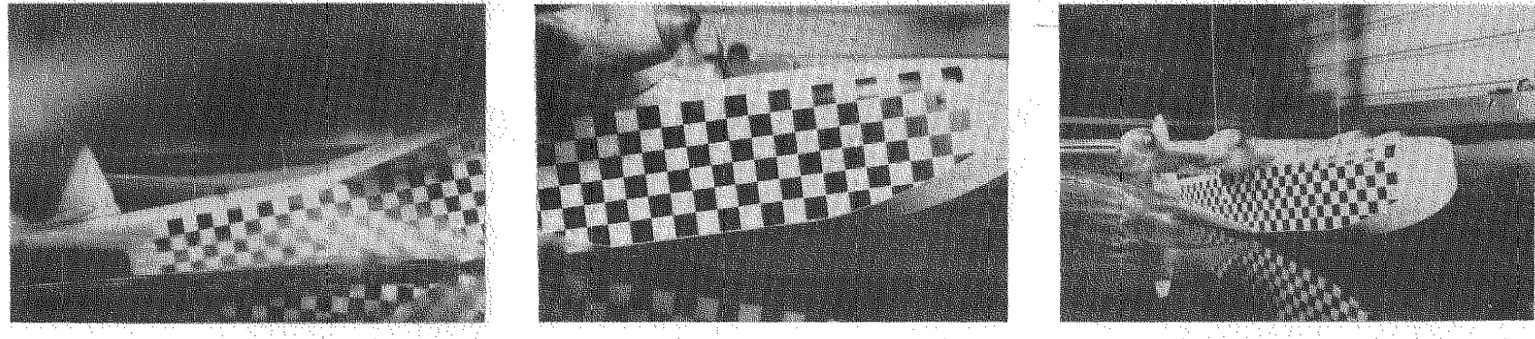

(c)
$\eta = -8°$
$C_v = 9{\cdot}10$
$\alpha_k = 7{\cdot}4°$

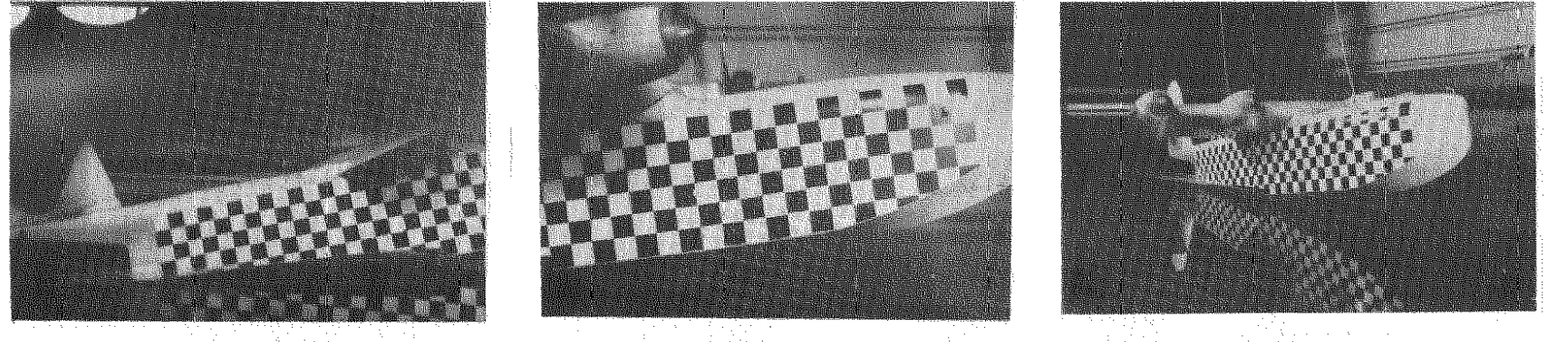

MODEL A

SPRAY PHOTOGRAPHS WITH TAKE-OFF POWER (2)

FIG. 12a (2)

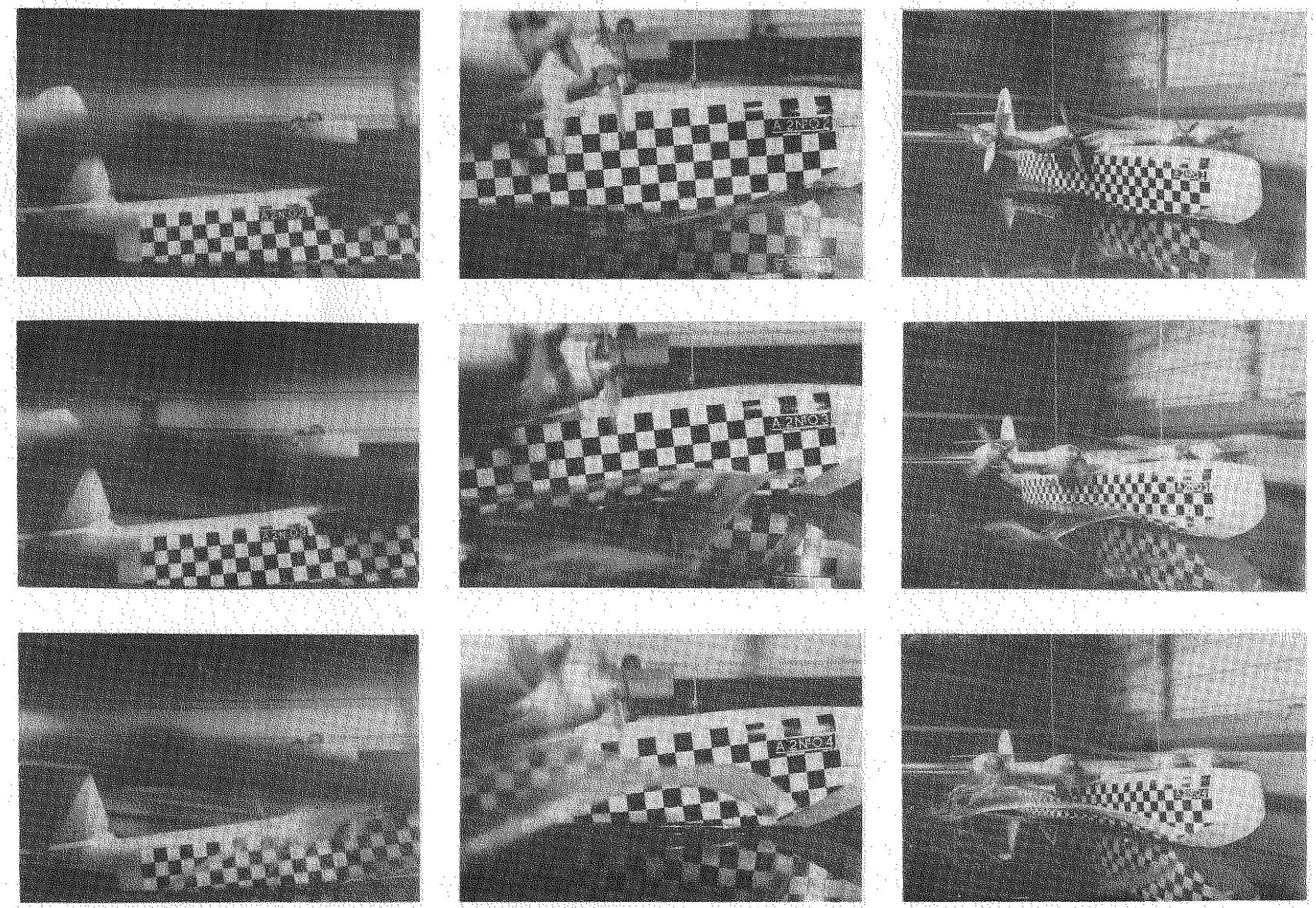

MODEL A

SPRAY PHOTOGRAPHS WITH PROPELLERS WINDMILLING (1)

FIG. 12b (1)

FIG. 12b (2)

MODEL A

SPRAY PHOTOGRAPHS WITH PROPELLERS WINDMILLING (2)

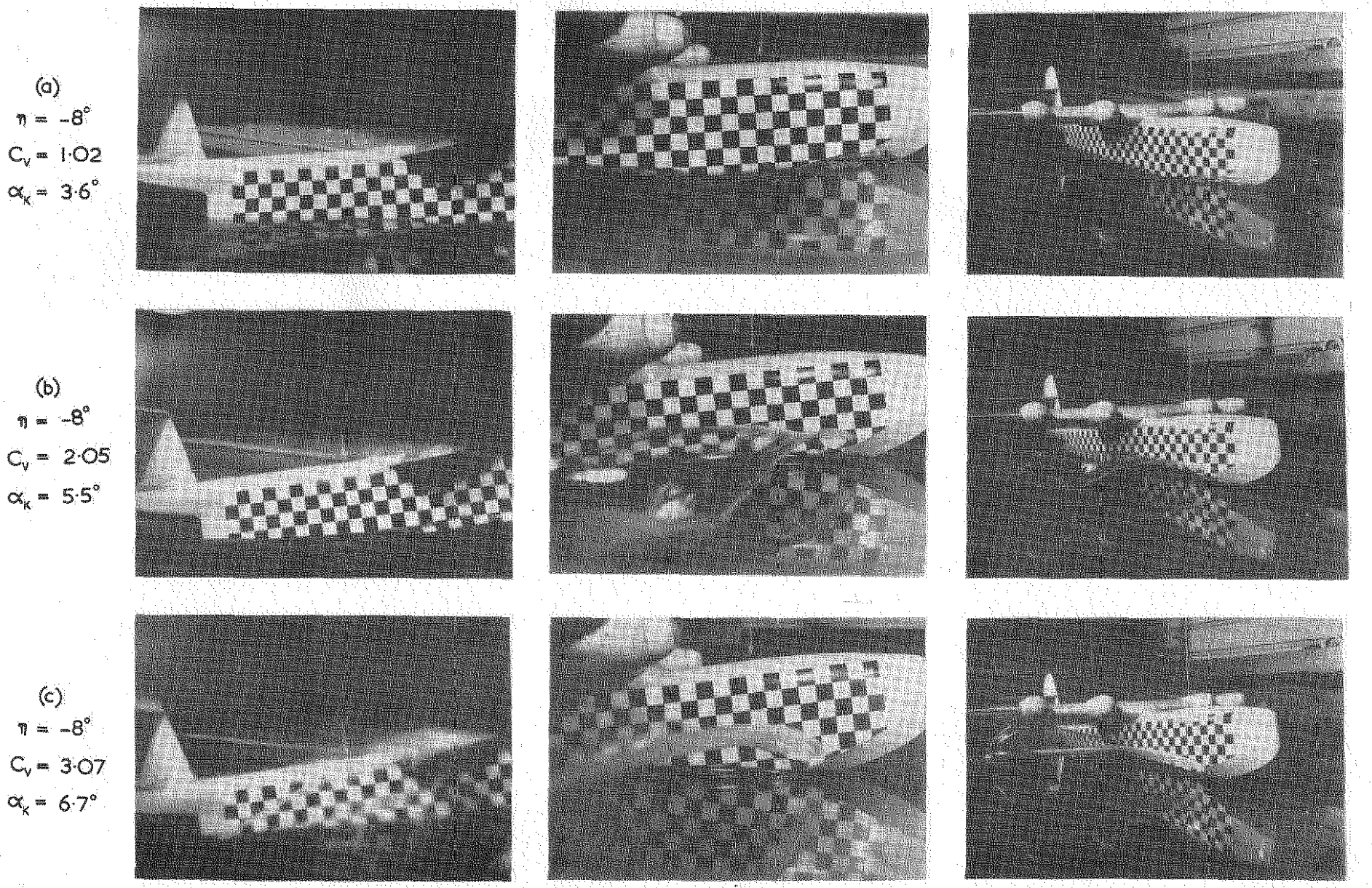

MODEL A

SPRAY PHOTOGRAPHS WITH FAIRINGS (1)

FIG. 12c (1)

(a)
$\pi = -8°$
$C_v = 4{\cdot}09$
$\alpha_k = 10{\cdot}2°$

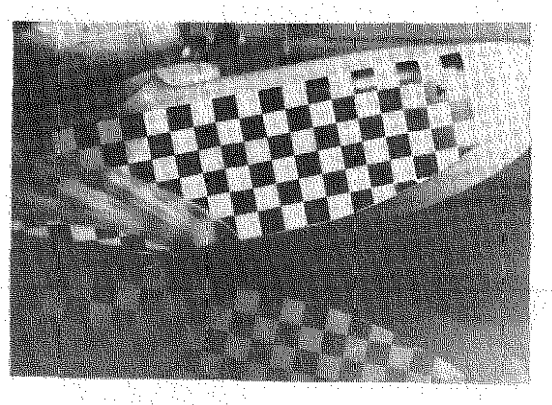

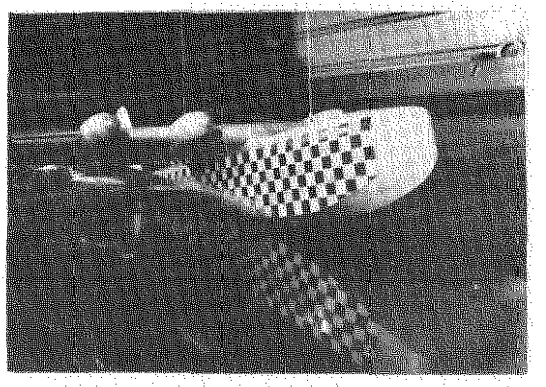

(b)
$\pi = -8°$
$C_v = 5{\cdot}12$
$\alpha_k = 11{\cdot}0°$

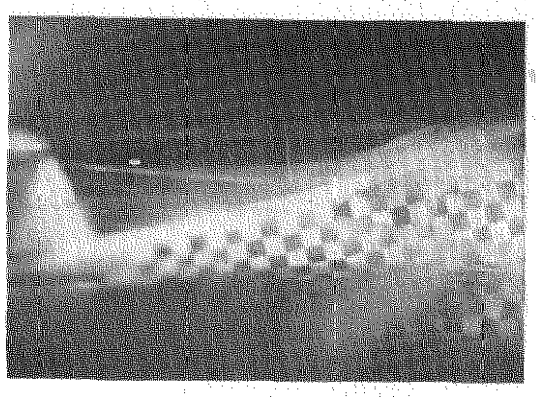

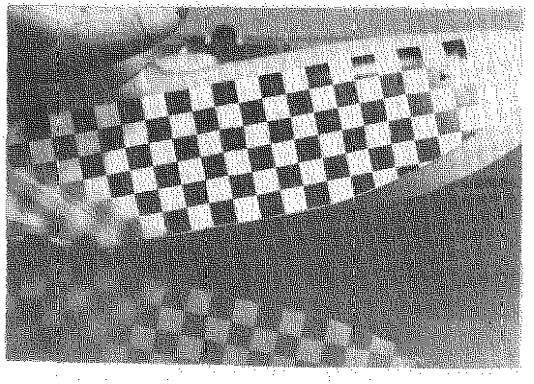

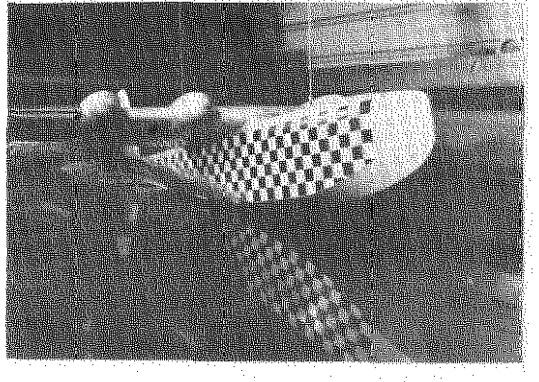

(c)
$\pi = -8°$
$C_v = 9{\cdot}21$
$\alpha_k = 10{\cdot}1°$

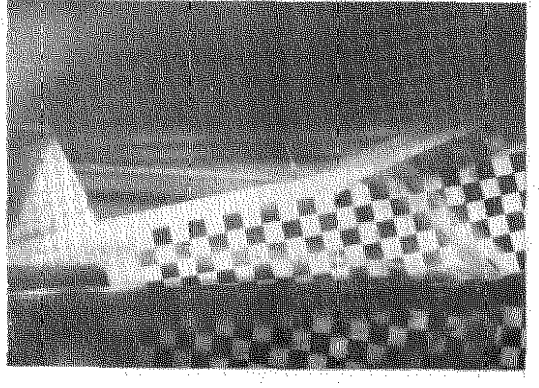

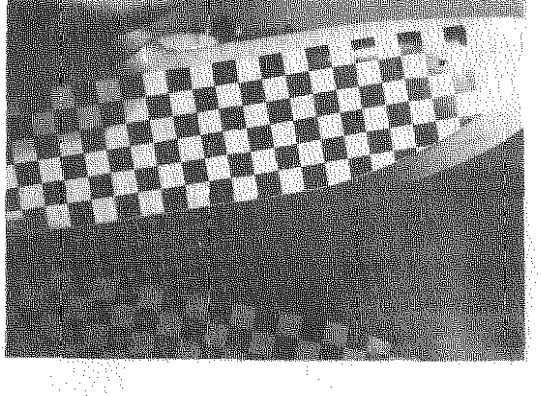

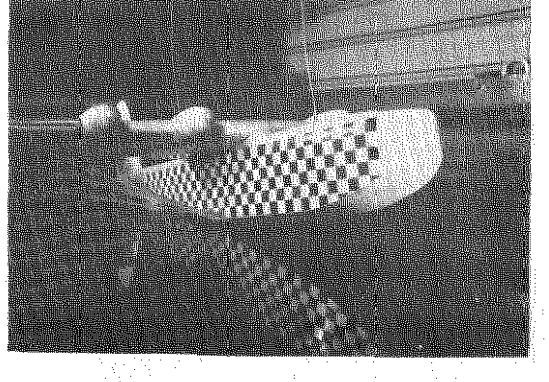

MODEL A

SPRAY PHOTOGRAPHS WITH FAIRINGS (2)

FIG. 12c (2)

FIG.14a.

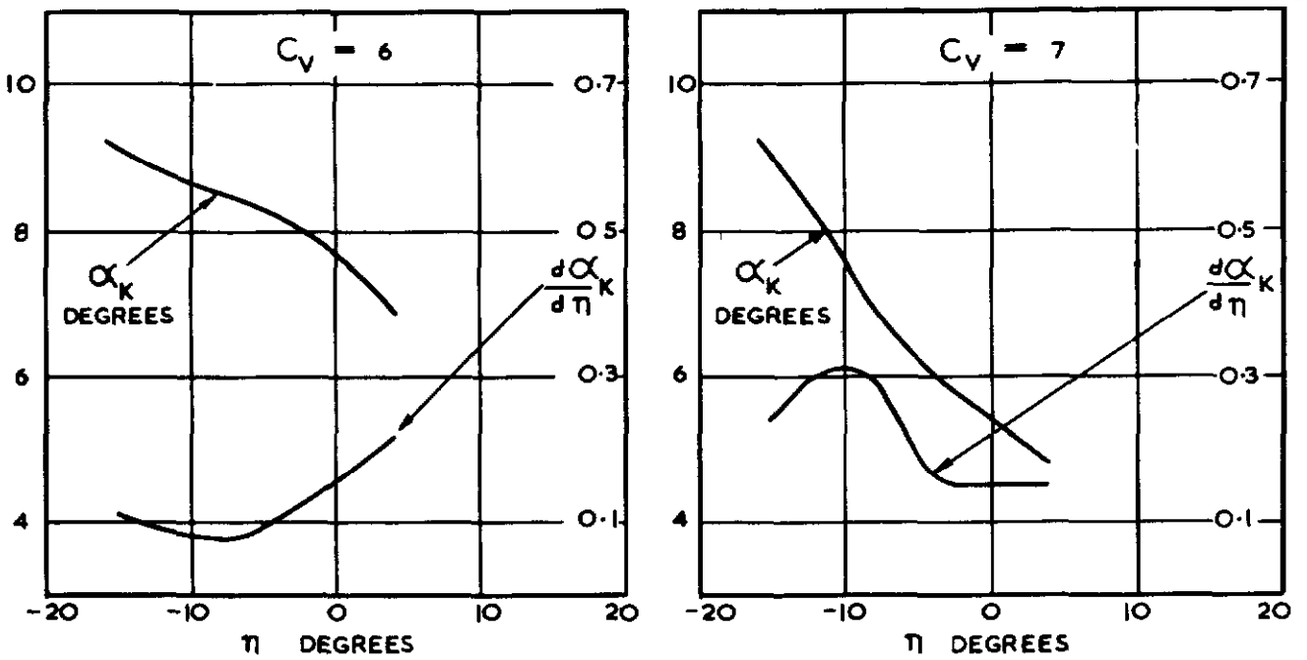

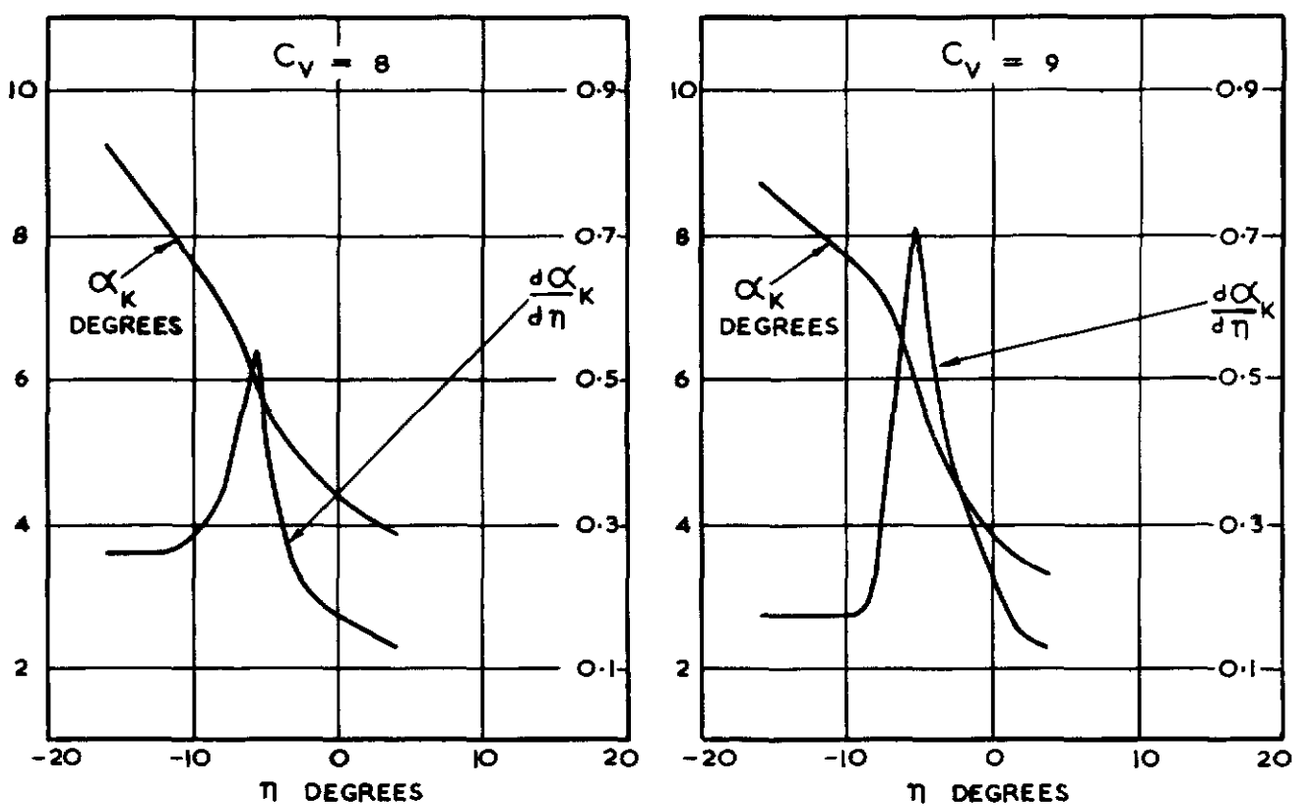

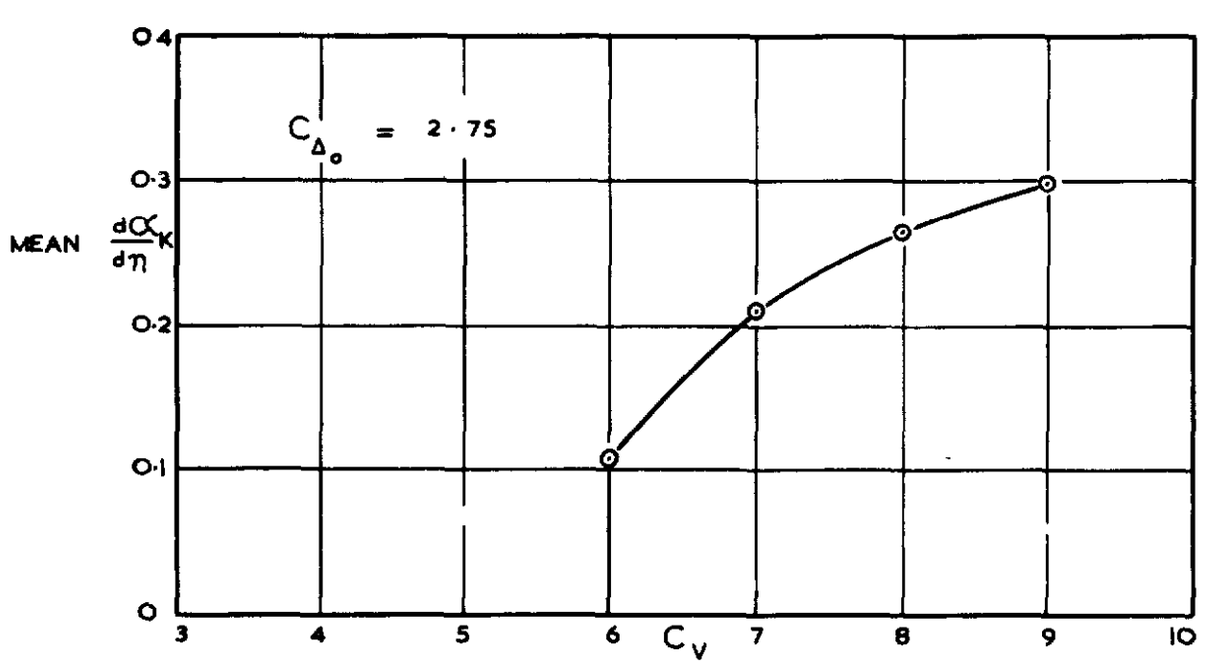

MODEL A

ELEVATOR EFFECTIVENESS WITH TAKE-OFF POWER

FIG.14 b.

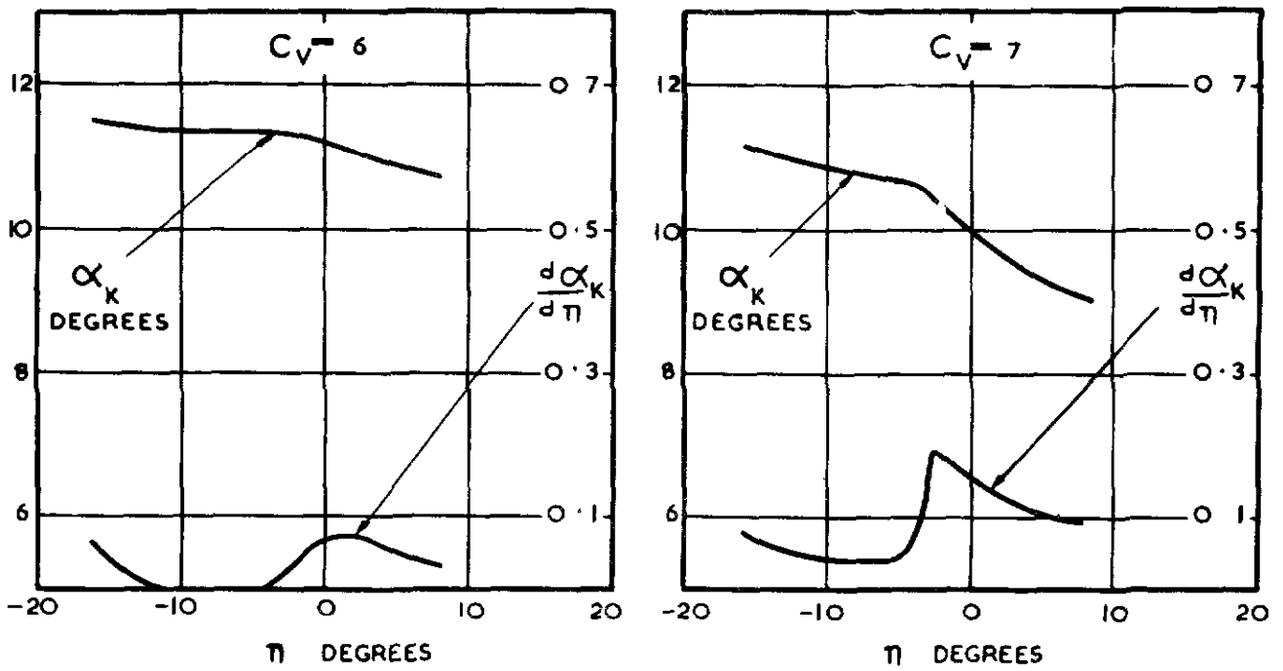

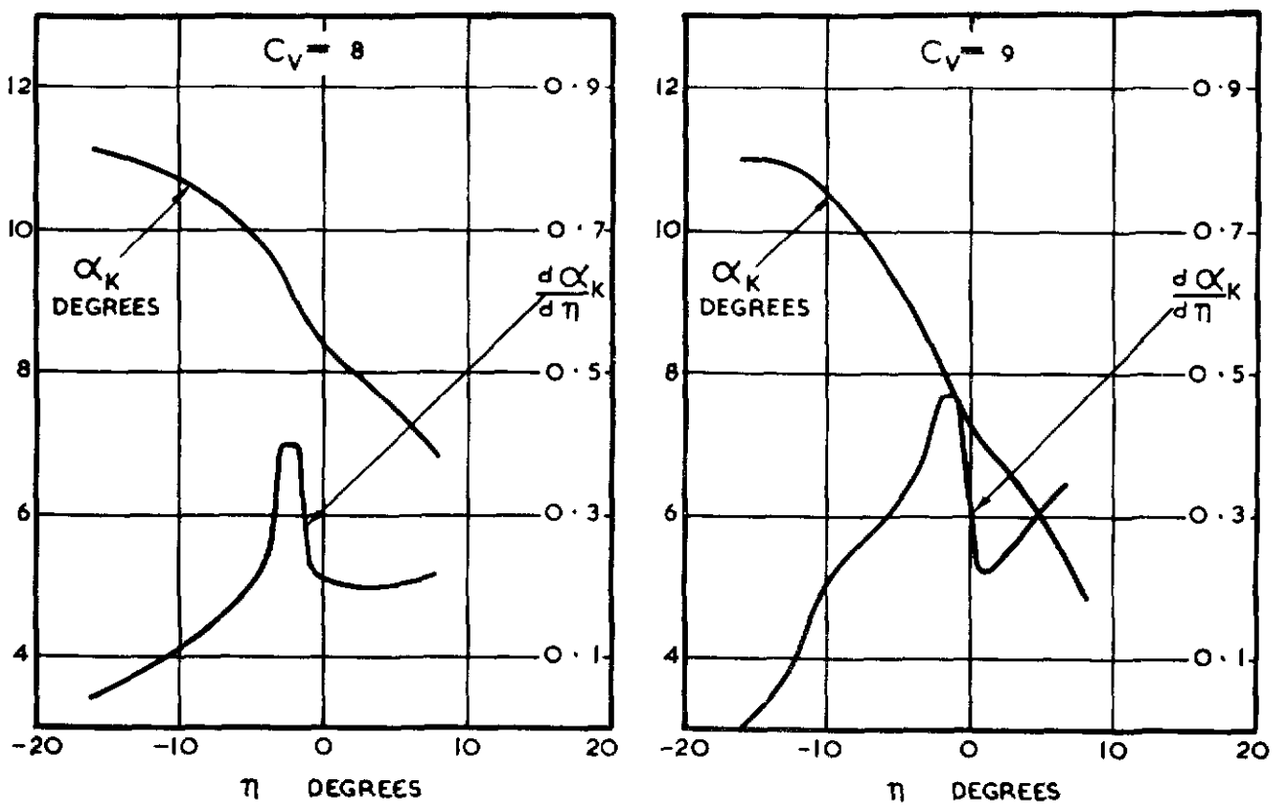

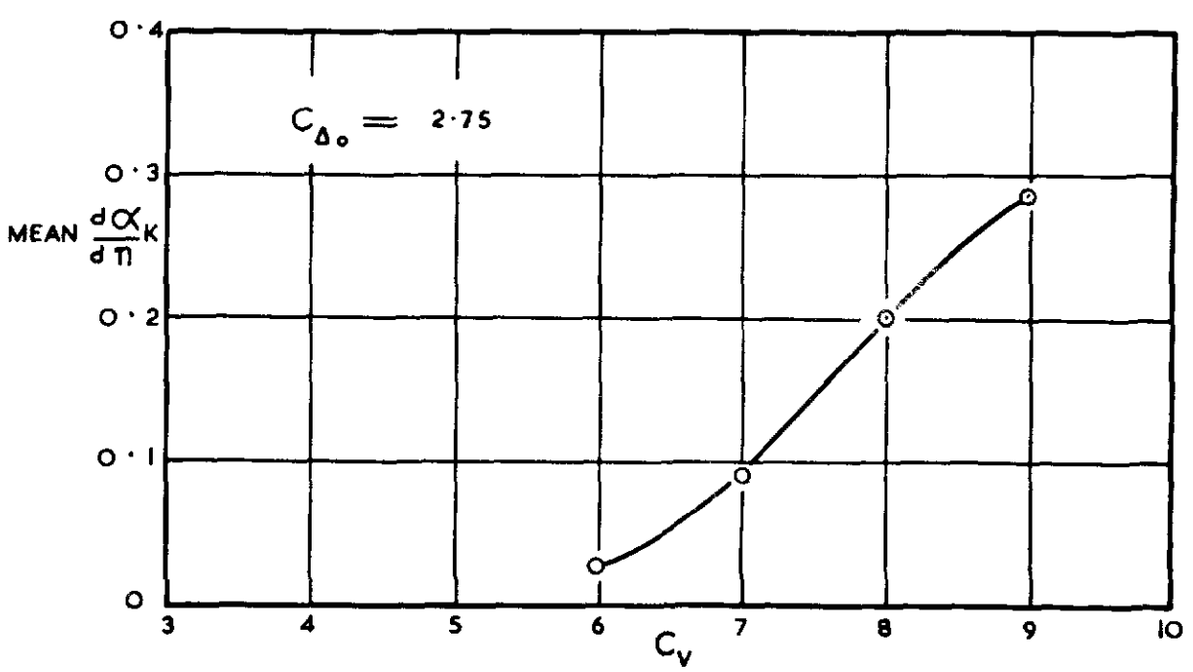

MODEL A

ELEVATOR EFFECTIVENESS WITH PROPELLERS WINDMILLING

FIG.14c.

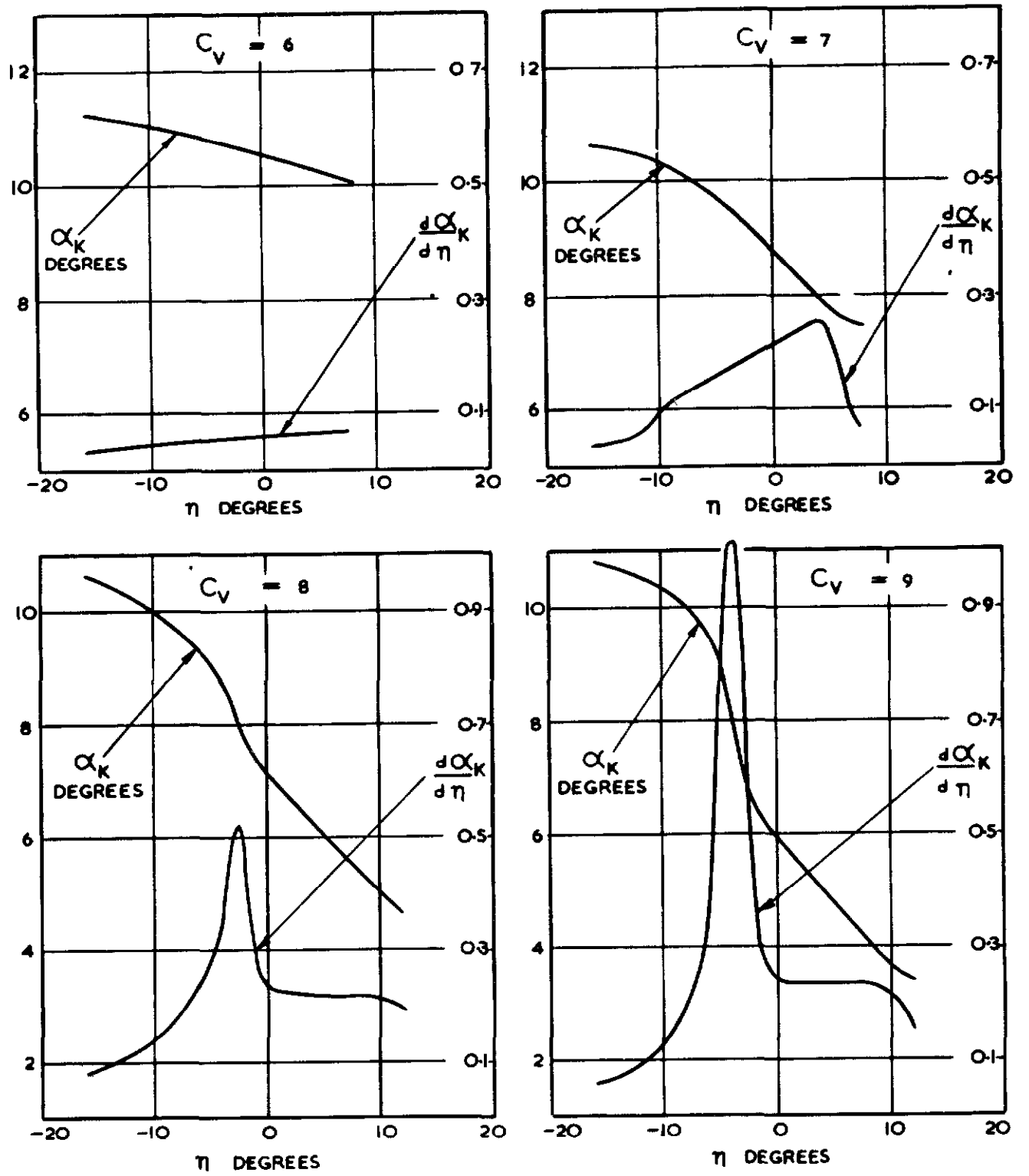

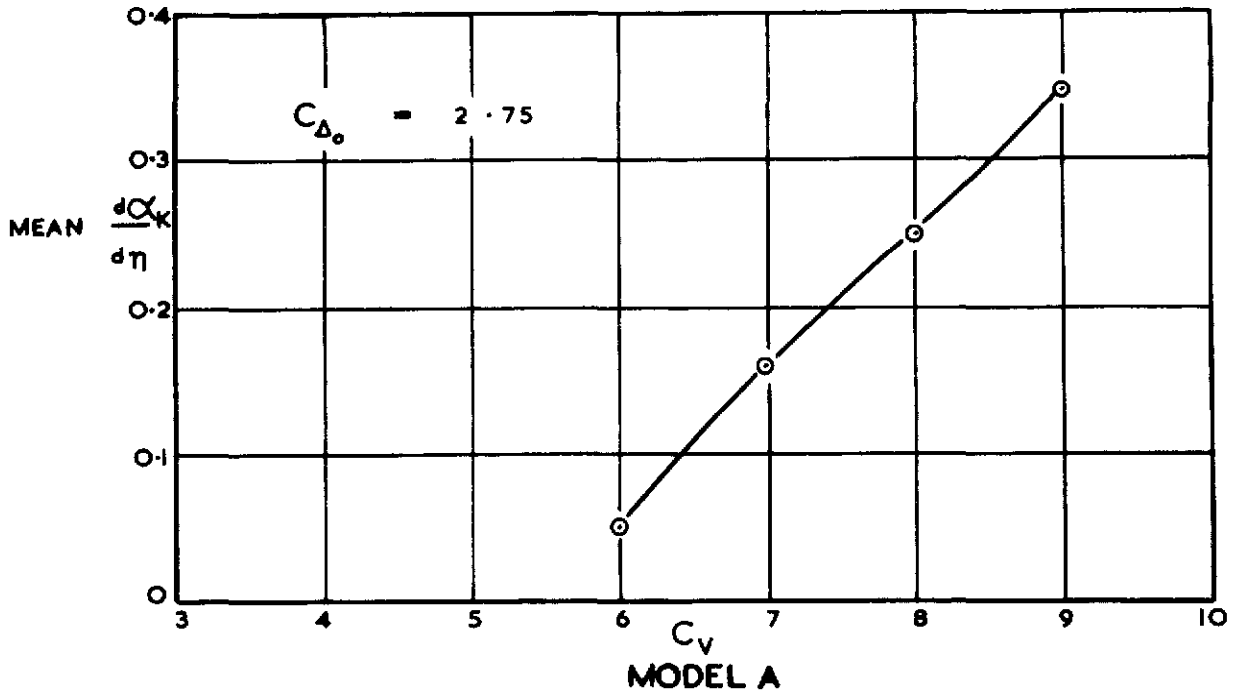

MODEL A

ELEVATOR EFFECTIVENESS WITH FAIRINGS

FIG.14d.

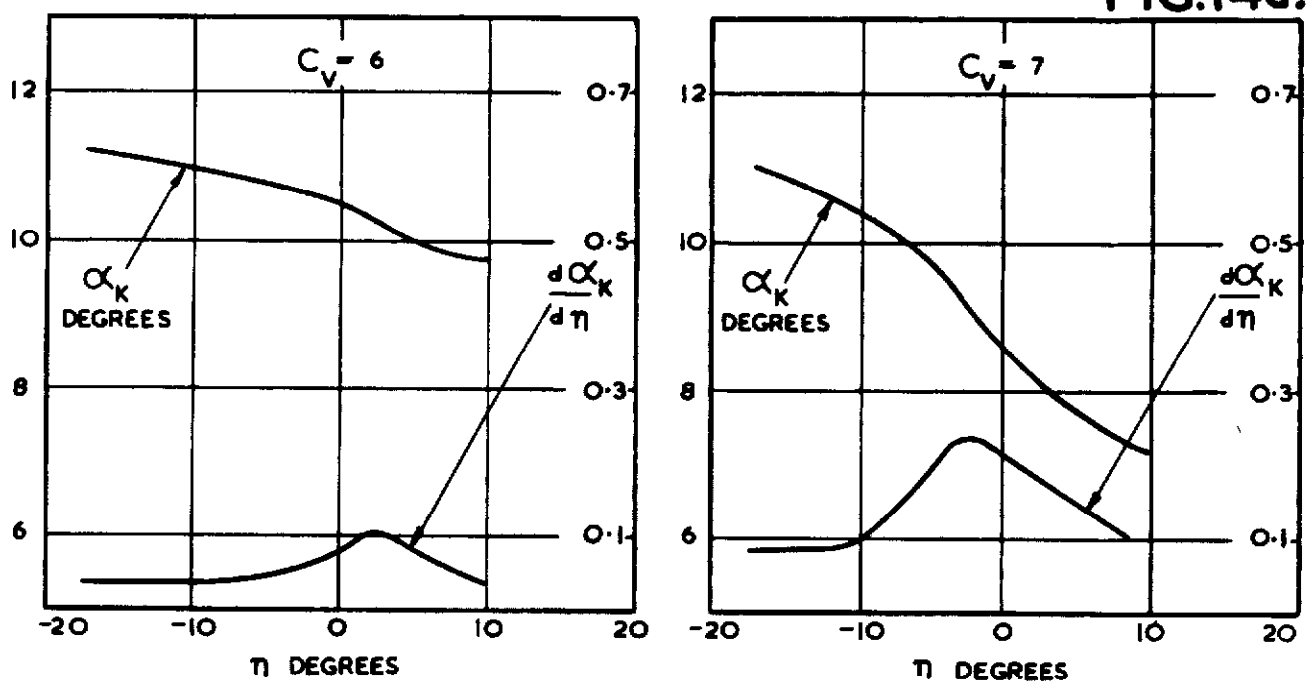

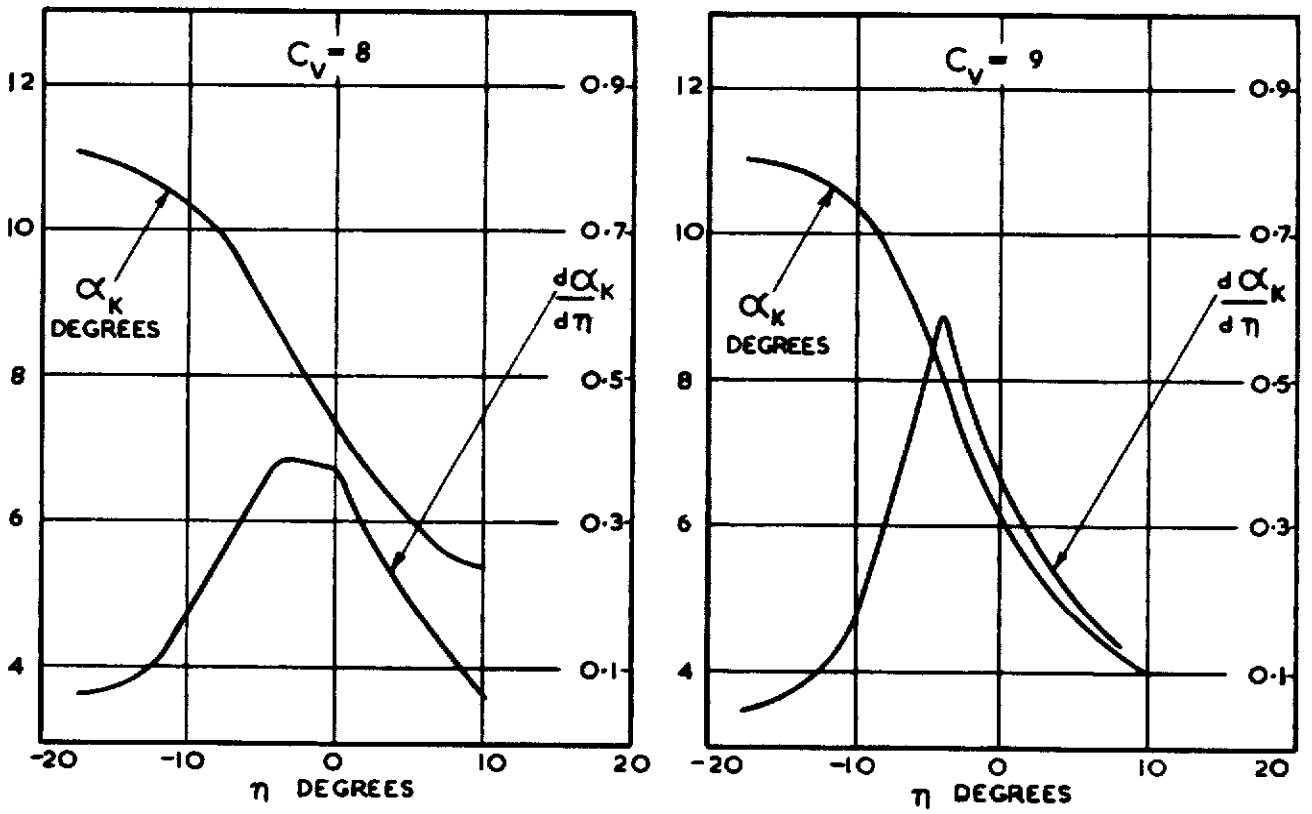

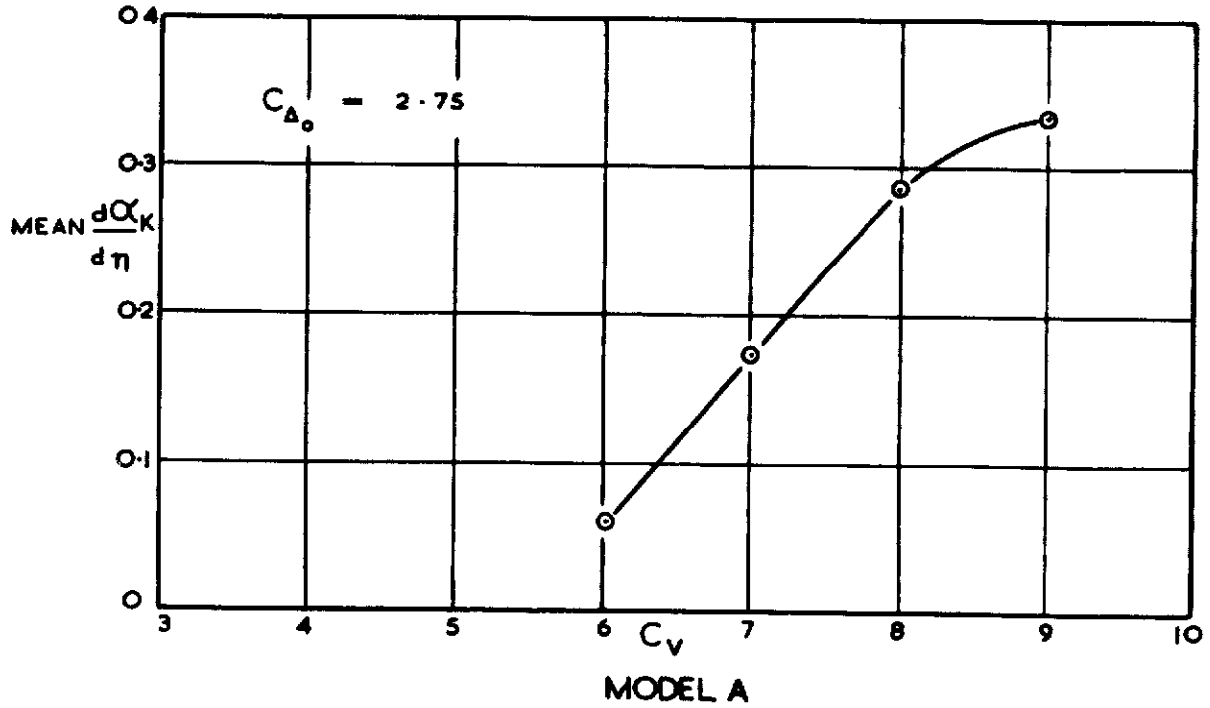

MODEL A
ELEVATOR EFFECTIVENESS WITH FULL SPAN SLATS

FIGS. 15 & 16.

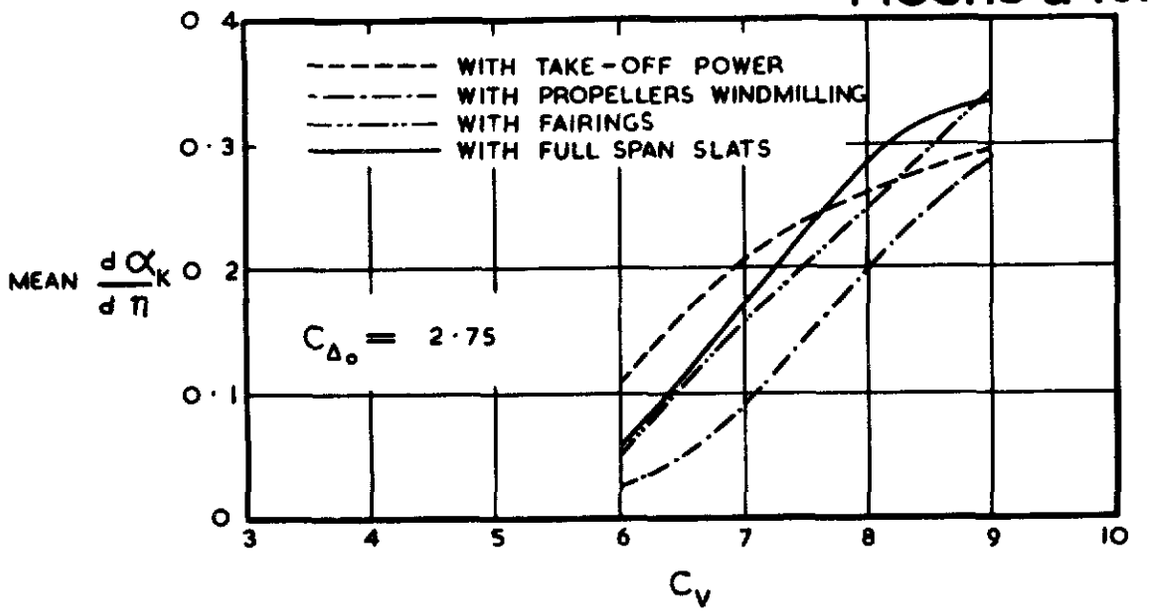

FIG. 15. COMPARISON OF ELEVATOR EFFECTIVENESS

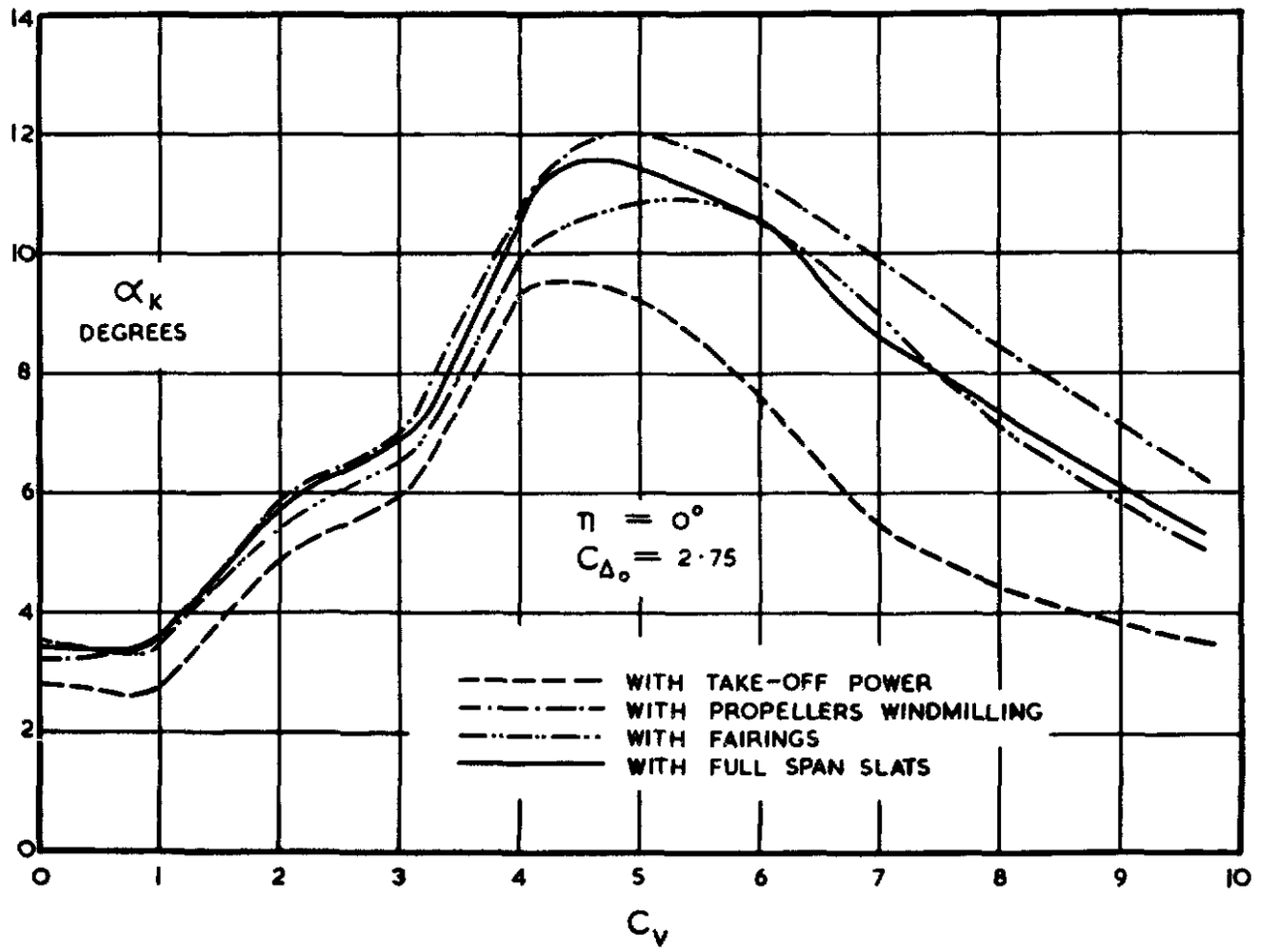

FIG. 16. COMPARISON OF TRIM CURVES

Printed and published by
HER MAJESTY'S STATIONERY OFFICE

To be purchased from
York House, Kingsway, London W.C.2
423 Oxford Street, London W.1
13A Castle Street, Edinburgh 2
109 St Mary Street, Cardiff
39 King Street, Manchester 2
Tower Lane, Bristol 1
2 Edmund Street, Birmingham 3
80 Chichester Street, Belfast
or through any bookseller

Printed in Great Britain

S.O. Code No. 23-9010-49